Phosphorylation of a reinitiation supporting protein, RISP, determines its function in translation reinitiation

Eder Mancera-Martínez[1,†], Yihan Dong[1,†], Joelle Makarian[1], Ola Srour[1], Odon Thiébeauld[1], Muhammed Jamsheer[1], Johana Chicher[2], Philippe Hammann[2], Mikhail Schepetilnikov [ID][1] and Lyubov A. Ryabova [ID][1,*]

[1]Institut de biologie de moléculaire des plantes UPR2357 du CNRS, Université de Strasbourg, Strasbourg, France and [2]Plateforme protéomique Strasbourg Esplanade FRC1589 du CNRS, Université de Strasbourg, Strasbourg, France

ABSTRACT

Reinitiation supporting protein, RISP, interacts with 60S (60S ribosomal subunit) and eIF3 (eukaryotic initiation factor 3) in plants. TOR (target-of-rapamycin) mediates RISP phosphorylation at residue Ser267, favoring its binding to eL24 (60S ribosomal protein L24). In a viral context, RISP, when phosphorylated, binds the CaMV transactivator/ viroplasmin, TAV, to assist in an exceptional mechanism of reinitiation after long ORF translation. Moreover, we show here that RISP interacts with eIF2 via eIF2β and TOR downstream target 40S ribosomal protein eS6. A RISP phosphorylation knockout, RISP-S267A, binds preferentially eIF2β, and both form a ternary complex with eIF3a *in vitro*. Accordingly, transient overexpression in plant protoplasts of RISP-S267A, but not a RISP phosphorylation mimic, RISP-S267D, favors translation initiation. In contrast, RISP-S267D preferentially binds eS6, and, when bound to the C-terminus of eS6, can capture 60S in a highly specific manner *in vitro*, suggesting that it mediates 60S loading during reinitiation. Indeed, eS6-deficient plants are highly resistant to CaMV due to their reduced reinitiation capacity. Strikingly, an eS6 phosphomimic, when stably expressed in eS6-deficient plants, can fully restore the reinitiation deficiency of these plants in cellular and viral contexts. These results suggest that RISP function in translation (re)initiation is regulated by phosphorylation at Ser267.

INTRODUCTION

Translation initiation—the rate-limiting step of protein synthesis in eukaryotes—requires rapid assembly of a 43S preinitiation complex (43S PIC) composed of at least eukaryotic initiation factor 3 (eIF3), eIF5, eIF1, eIF1A, the eIF2•GTP•Met–tRNAi^{Met} ternary complex (TC) attached to the 40S ribosomal subunit (40S) (1–3). eIF3 comprises 13 distinct subunits in mammals and plants—eIF3a–eIF3m (4,5), and stimulates binding of Met–tRNAi^{Met} to 43S PIC via the eIF2β subunit of a heterotrimer eIF2 made up of eIF2α, β and γ subunits (6,7). Through its cap-binding subunit 4E (eIF4E), the eIF4F complex binds the m7G cap structure of mRNA, and, together with eIF3, promotes loading of 43S PIC on the mRNA 5′-end, resulting in formation of the 48S PIC. Many studies have suggested that establishment of a network of multiple interactions among initiation factors is required to facilitate mRNA recruitment to the 48S PIC (2). Recent data uncovered m7G cap interacting domains within eIF3 subunits d (eIF3d) (8) and l (eIF3l) (9) that may play roles in eIF4E-independent mRNA recruitment to m7G cap, if the m7G cap is anchored by eIF3. A number of accessory proteins implicated in binding initiator tRNA to 40S-mRNA have been identified (10). After 43S PIC scanning along the mRNA leader and codon–anticodon complex formation at the optimal AUG codon, 60S joins and elongation begins. In plants, the translation machinery is largely conserved; however, eIFs such as eIFiso4E and eIFiso4G, forming an eIFiso4F complex, determine plant specificity (3). Plant accessory or regulatory proteins orchestrating translation initiation are largely unknown, and it is only recently that investigations have shed light on the roles of some of these factors (11,12).

After translation termination, posttermination complexes are split by ribosome recycling factors ABCE1 and eRF1 into 60S and tRNA/mRNA-associated 40S subunits (13). Frequently, after terminating translation, the 40S subunit can resume scanning and reinitiate at downstream AUGs. The reinitiation competence of ribosomes depends on the duration of elongation, and thus occurs mainly after translation of short upstream ORFs (uORFs) (14). In such cases, some eIFs, mainly eIF3, may remain transiently associated with ribosomes through the short elongation and termination events, and assist 40S scanning and *de novo* recruitment of Met-tRNAi[Met] and/or the 60S ribosomal subunit (15).

uORFs are common in mammals and plants, being present in at least 30–45% of full-length mRNAs (16,17); many of these uORFs are translated (18). Through its role in the stimulation of translation initiation in eukaryotes, eIF3, has also been implicated in translation reinitiation in eukaryotes (15,19–23). In plants, eIF3h ensures that a fraction of uORF-translating ribosomes retain competence to resume scanning and reinitiate translation at downstream ORF (21). In mammals and yeast, the two noncanonical initiation factors—subunits of the heterodimeric complex DENR-MCT-1 (MCTS1 in human)—function in reinitiation after short ORF translation as *trans*-acting factors that bind tRNA (24,25).

In eukaryotes, the target of rapamycin (TOR) signaling pathway integrates nutrient and energy sufficiency, hormones and growth factors to provide additional levels of translation initiation control, mainly via phosphorylation of eIF4E-binding proteins (4E-BPs) and kinases of the 40S ribosomal protein S6 (S6Ks) (26–28). Although 4E-BP-like proteins have not yet been found in *Arabidopsis* (28), *Arabidopsis* TOR, when activated by the plant hormone auxin in a small GTPase ROP2 (Rho of Plants 2) dependent manner, promotes translation reinitiation of mRNAs that harbour uORFs within their leader regions by phosphorylating eIF3h, which bolsters the reinitiation capacity of postterminating ribosomes, although the underlying molecular mechanisms remain enigmatic (29,30).

Reinitiation after translation of a long ORF is rare, but does occur in specific circumstances. For example, it is activated in *Cauliflower mosaic virus* (CaMV) by a single viral protein transactivator/viroplasmin (TAV) (19,31,32). Here, TAV, expressed from the 19S subgenomic RNA, is crucial for translation of the polycistronic 35S RNA (which contains seven long ORFs) via a reinitiation mechanism (33). TAV promotes retention of eIF3 and reinitiation supporting protein (RISP) on polysomes throughout longer elongation to ensure resumption of scanning and subsequent reinitiation events on the 35S mRNA or artificial bicistronic mRNA in dicotyledons (19,33). TAV physically binds TOR and promotes its activation via an as yet unknown mechanism. Accordingly, RISP reinitiation activity is controlled by S6K1 phosphorylation on a unique site (S267 in the *Arabidopsis* sequence) (33). Active TOR binds polyribosomes concomitantly with polysomal accumulation of TAV, eIF3 and RISP, with RISP being phosphorylated.

In planta, endogenous RISP has been detected within 40S and 80S ribosomes, while exogenous RISP joins 60S, but not 80S (34). It can therefore be anticipated that RISP sequestration by 80S negatively impinges upon subunit joining. Different cellular interaction partners have been assigned to RISP, including core eIF3 subunits a and c and the 60S ribosomal protein L24 (eL24) (34). RISP phosphorylation appears to promote its binding to eL24, whereas, the non-phosphorylated form of RISP preferentially binds eIF3c (33). In addition, RISP can be specifically co-immunoprecipitated not only with endogenous eIF3c, but also eIF2α and eS6 in soluble cell extracts (33). These characteristics likely assign different functions to RISP in translation, but the mechanisms are not clear.

Here, we identify two novel RISP partners: eIF2β and the 40S ribosomal protein S6 (eS6). To identify the mechanism(s) by which RISP regulates translation *in planta*, we characterized RISP interactions with its partners *in vitro* and *in planta*. We demonstrated that non-phosphorylated RISP might enhance 43S PIC formation by interacting with both eIF3 and eIF2, while phosphorylated RISP can mediate binding of eS6 and 60S to promote translation reinitiation. In this paper we provide evidence that eS6—the most studied target of TOR/S6K1 signaling—can play a role in translation reinitiation.

MATERIALS AND METHODS

Plant materials and growth conditions

Arabidopsis thaliana ecotype Columbia (Col-0) was used as the wild-type model in this study. SALK_048825 (*rps6a*) and SALK_012147 (*rps6b*) lines were kindly provided by Dr Thierry Desnos (CEA-Université Aix-Marseille-II, Marseille, France); all have a Col-0 background. Genotype details of these lines are described in (35). *rispa Arabidopsis* line was described (34). *rps6a* line was transformed by the floral dip method with either p*GWB2-eS6B*, or p*GWB2-eS6B-S237A/S240A/S241A*, or p*GWB2-eS6B-S237D/S240D/S241D,* or p*GWB5-eS6B-cMyc*. Then *rps6a/S6B, rps6a/S6B*[S/D] and *rps6a/S6B*[S/A] homozygous lines were screened based on hygromycin resistance. The *rispa* line was transformed with p*GWB5-RISP-GFP*, and two *rispa/RISP-GFPox* homozygous lines ectopically expressing RISP-GFP were isolated based on hygromycin resistance.

CaMV infection

Virus infection was achieved using an agroinfectible construct derived from WT CaMV isolate CM1841 (designated in this study simply as CaMV) and kindly provided by Dr Kappei Kobayashi (36,37). Antibodies against His-TAV were described in (34) and against CaMV CP were kindly provided by Dr M. Keller.

Assay for root gravitropism

Seedlings were germinated vertically in the dark at 22°C for 4 days. The plates were then turned through 90°. Curvature in root gravitropic response was analyzed 24 h after gravity stimulation.

Protoplast assays

p*shortGUS* (or p*monoGUS*) and p*monoGFP* were described previously (33) and p*ARF5-GUS* (29). PCR product corresponding to AteIF2β was amplified from eIF2β cDNA (At5g20920) with pairs of specific primers and cloned into p*monoGUS* to replace GUS and obtain the p*eIF2β* construct. The RISP coding sequence was subcloned under the control of the *CaMV* 35S promoter into p*TAV* (p35S-P6) (34) to obtain p*RISP*. p*RISP-S267A* and p*RISP-S267D* were generated by substitution of Ser at the position 267 to Ala (S267A) and Asp (S267D), respectively, within RISP ORF by site-directed PCR mutagenesis. Protoplasts from *Arabidopsis* suspension cell cultures and mesophyll protoplasts from 2-week WT, *rps6a, rps6a/S6B^{S/D}* or *rps6a/S6B^{S/A}* plantlets were transfected with plasmid DNA by the PEG method (38). Five microgram p*monoGFP* and either 5 μg p*shortGUS* or p*ARF5-GUS*, without or with increasing concentrations of p*RISP* (or phosphorylation mutants of RISP) and/ or p*eIF2β* as indicated were used for cotransformation of *Arabidopsis* suspension culture protoplasts (Figure 2C, D). Five microgram p*monoGFP* and (1) 5 μg p*shortGUS* or (2) 10 μg p*ARF5-GUS*, or two pairs of plasmids—(3) 10 μg p*biGUS* (39) and 10 μg p*35S* or (3/4) 10 μg p*biGUS* and p*TAV* (p35S-P6) (40) were used to transform mesophyll protoplasts prepared from WT, *s6a, s6a/S6B^{S/D}* or *s6a/S6B^{S/A} Arabidopsis* (Figure 4C). After over-night incubation at 26°C in WI buffer (4 mM MES pH 5.7, 0.5 M Mannitol, 20 mM KCl) transfected protoplasts were harvested by centrifugation and protein extract was prepared in GUS extraction buffer (50 mM NaH₂PO₄ pH 7.0, 10 mM EDTA, 0.1% NP-40). The aliquots were immediately taken for GUS reporter gene assays. GUS activity was measured by a fluorimetric assay using a FLUOstar OPTIMA fluorimeter (BMG Biotech) (41). pmonoGFP expression was monitored by western blot using anti-GFP antibodies (Chromotek) and/ or by determining GFP fluorescence. Both GFP fluorescence and β-glucuronodase functional activity were analysed in the same 96-well microtiter plate. The values given are the means from at least three independent experiments. GUS mRNA levels after protoplasts incubation were determined as indicated in Supplementary information.

GST pull-down assay

PCR products corresponding to RISP, eIF3aΔ (aa 1–646), eIF2β and eS6 C-ter (CS6) were inserted into pGEX-6P1 (Pharmacia Biotech) as in-frame fusions with glutathione-*S*-transferase, GST. The *in vitro* GST pull-down assay was performed as described previously (19). GST pull-down assays were set up as follows: molar equivalents of purified proteins were incubated with the immobilized GST or GST-tagged protein at 4°C for 2 h under constant rotation. Binding of GST or GST-RISP to wheat eIF2, GST or GST-RISP to His-eIF2β, GST or GST-eIF2β to RISP phosphorylation mutants, and GST or GST-eIF3a to His-eIF2β was carried out in a 300 μl reaction containing 50 mM HEPES pH 7.5, 100 mM KCl, 3 mM magnesium acetate, 0.1 mM EDTA, 0.5% v/v Igepal 360® (Sigma-Aldrich®) and cOmplete® protease inhibitor cocktail

(Roche®). Sepharose beads and associated proteins (bound fraction, B) were recovered by centrifugation at 500g for 5 min and thoroughly washed as before (4 washing steps). Fifty microliters of the first unbound fraction (U) solution and bound fraction were used for SDS-PAGE analysis. Binding of GST or GST-eIF3a (—GST or GST-CS6—) to RISP phosphorylation mutants—RISP-S267A or RISP-S267D—was carried out in 3-fold increased reaction mixture (900 μl) overnight at 4°C. After intensive washing, GST-eIF3a-RISP-S267A or GST-eIF3a-RISP-S267D complexes were split into three equal fractions, washed and used for incubation with or without eIF2β, 70 pmol (purified 60S ribosomal subunits, respectively, 100 pmol) during 2 h at 4°C. eIF2β- or 60S-bound complex formation was analyzed, where the bound fractions (B) as well as 50 μl of the unbound fraction (U) were separated by a 12% SDS-PAGE gel and stained by Coomassie™ blue.

Polysome profiling

Polyribosomes were obtained from *A. thaliana* seedlings and analysed as described previously (42). Crude polysomal extracts were obtained from 200 mg of *Arabidopsis* seedlings treated or not with 1 μM auxin during 24 h and resolved on 7–47% sucrose gradient centrifuged for 3 h at 38 000 rpm (rotor SW41-Ti, Beckman Coulter). Analysis of polysome profiles was performed with an absorbance detector at 254 nm and sucrose gradients collected with a BioLogic Duoflow fractions collector (Biorad) into 18 fractions of 500 μl each. Samples from the light (LP), heavy polysome (HP) and non-polysomal 80S, 60S and 40S (NP) fractions were then separated on a 12.5% SDS-PAGE followed by immunoblotting to determine total and phosphorylated RPS6 and RISP protein levels. Rabbit polyclonal antibodies raised against RISP and eL13 were described previously (34) and (43), respectively. Polyclonal Phospho-(Ser/Thr)Akt substrate (RxRxxS/T) antibody for RISP-P detection was from Cell Signaling Technology. Antibodies against eS6 (RPS6) and phospho-specific antibodies against S240-P were generated by Agrisera, Umeå, Sweden and kindly provided by Albrecht G. von Arnim (University of Tennessee, Knoxville, USA). Polyclonal anti-eS14 was from Agrisera.

Protein purification

Wheat germ eIF2 was kindly provided by K. Browning (University of Texas at Austin, USA). GST-fusion and His-tagged proteins were expressed in Rosetta 2 DE3 pLysS (Novagen®) and purified using Glutathione Sepharose4B beads or HisTrap HP columns (GE Healthcare®), according to supplier protocol.

Yeast two-hybrid assay

PCR products corresponding to eIF2α, β and γ subunits were amplified from eIF2α (AT5G05470.1), eIF2β (AT5G20920.1) and eIF2γ (AT1G04170.1) cDNAs with pairs of specific primers and cloned into the pGBKT7 vector (Clontech®) as in-frame fusion with the BD-domain

to obtain the pBD-eIF2 subunit variants. eIF2β and eS6 deletion mutants fused to the BD-domain in the pG-BKT7 vector were produced by deletion mutagenesis of the pGBK-eIF2β and eS6 (AT5G10360.1) cDNA. RISP (AT5G61200.3) and its deletion mutants fused to AD were produced by PCR from the original pGAD-RISP (34) and cloned between the NdeI and BamHI sites of pGADT7 (Clontech®). PCR product corresponding to RISP-S267D and RISP-S267A were generated by substitution of Ser at position 267 to Asp (S267D) or to Ala (S267A) from pGAD-RISP by site-directed PCR mutagenesis and cloned into pGADT7 vector to obtain the pGAD-RISP-S267D and pGAD-RISP-S267A constructs.

Yeast two-hybrid protein interaction assays were performed according to (33). Constructs containing GAL4 AD-domain and BD-domain fusion variants were co-transformed into AH109 cells. Transformants were selected onto SD-Leu-Trp plates. Surviving yeast colonies were picked as primary positives and transferred on SD-Leu-Trp-Ade selection plates to score protein interaction. β-Galactosidase activity was measured by using the Gal-Screen® assay system (Tropix® by Applied Biosystems®) The values given are the means from more than three independent experiments. Yeast expression levels of all the BD- and AD-fusion variants were monitored by immunoblot analysis with anti-HA (Sigma-Aldrich®) and anti-cMyc (Santa-Cruz Biotechnology®) antibodies of yeast cell lysates using a rapid urea/SDS lysis procedure (data not shown).

Mass spectrometry analysis

Samples were prepared for mass-spectrometry analyses as described (44). Briefly, samples solubilized in Laemmli buffer were precipitated with 0.1 M ammonium acetate in 100% methanol. After a reduction-alkylation step (Dithiothreitol 5 mM, Iodoacetamide 10 mM), proteins were digested overnight with 1/25 (w/w) of sequencing-grade porcin trypsin (Promega). The peptide mixtures were resolubilized in water containing 0.1% FA (solvent A) before being injected on nanoLC–MS/MS (NanoLC-2DPlus system with nanoFlex ChiP module; Eksigent, ABSciex, Concord, Ontario, Canada), coupled to a TripleTOF 5600 mass spectrometer (ABSciex). Peptides were eluted from the C-18 analytical column (75 µm ID × 15 cm ChromXP; Eksigent) with a 5–40% gradient of acetonitrile (solvent B) for 90 min. Data were searched against a TAIR database containing the GFP-TOR sequence as well as decoy reverse sequences (TAIR10_pep_20101214). Peptides were identified with Mascot algorithm (version 2.2, Matrix Science, London, UK) through the ProteinScape 3.1 package (Bruker). They were validated with a minimum score of 30, a *P*-value <0.05 and proteins were validated respecting a false discovery rate FDR <1%.

Molecular model prediction

The 3D structural model of *Arabidopsis* RISP was created using RaptorX (45) and represented graphically by PyMOL (http://www.pymol.org).

RESULTS

RISP interacts with eIF2β and 40S ribosomal protein S6 (eS6) *in vitro*

Based on the observation that endogenous RISP can be specifically co-immunoprecipitated with not only endogenous eIF3c, but also eIF2α and eS6 in soluble cell extracts (34), we wondered whether RISP could physically associate with eIF2 and eS6. First, we assayed full-length RISP for direct binding to entire eIF2 purified from wheat germ in a GST pull-down assay (Figure 1A). All three eIF2 subunits were present in the bound fraction after incubation with GST-RISP, strongly indicating GST-RISP-eIF2 binding. Next, we tested the capacity of each eIF2 subunit to interact with RISP using the yeast two-hybrid (Y2H) assay (Figure 1B). Only subunit β, fused to the Gal4 binding domain (BD), interacted strongly with RISP fused to the Gal4 activation domain (AD-RISP), while α and γ were inactive, suggesting that subunit β is primarily responsible for eIF2 binding to RISP. Consistent with association of eIF2β and RISP in yeast, purified recombinant eIF2β and RISP interacted specifically in the GST pull-down assay (Figure 1C). To delineate regions of RISP involved in eIF2β binding, we performed a dissection based on a potential coiled-coil tertiary structure for RISP generated by RaptorX (45) (Figure 1D; right panel). RISP truncation and deletion mutants fused to the AD domain were tested to delineate regions important for binding to eIF2β. The N-terminal part of RISP (aa 1–190) binds eIF2β strongly, while the C-terminal part (aa 190–389) did not bind (Figure 2E). Binding was stronger between eIF2β and RISP lacking H1, but an internal deletion of H2 (aa 120–190) abolished RISP interaction with eIF2β. Thus, RISP domain H2 seems to be a key contact for eIF2 subunit β. Interestingly, the H2 helix has already been implicated in binding of eIF3 (34).

Sucrose density gradient sedimentation analysis of RISP binding to ribosomes showed that endogenous RISP was found associated stably with wheat germ high salt-washed 80S ribosomes and 60S ribosomal subunits, but not high salt-washed 40S subunits (34). Unexpectedly, Figure 1F demonstrates a highly specific interaction between AD-RISP and BD-eS6 under our Y2H conditions. In contrast to eIF2β, eS6 interacts exclusively with full-length RISP, indicating the probably critical importance of RISP tertiary structure for this interaction. We conclude that RISP interacts with eIF2β via its C-terminus, while only entire RISP can bind eS6 *in vitro*. However, RISP association with 40S in wheat germ extracts might be sensitive to high salt-washing conditions.

We next dissected eIF2β and eS6 regions based on their tertiary structures and positioning within the eIF2 complex or the 40S ribosomal subunit, respectively. A dissection of eIF2β was performed based on the archaebacterial aIF2β (46), which exhibits strong conservation with *Arabidopsis* eIF2β despite the fact that eIF2β has an N-terminal extension of 114 amino acids. The aIF2β N-terminal α-helix is connected by a flexible linker to a central α-β domain, followed by a zinc-binding domain at the C-terminus (aa 114–268; Figure 1G). Accordingly, the *Arabidopsis* eIF2β sequence was dissected into a C-terminal part, the N-
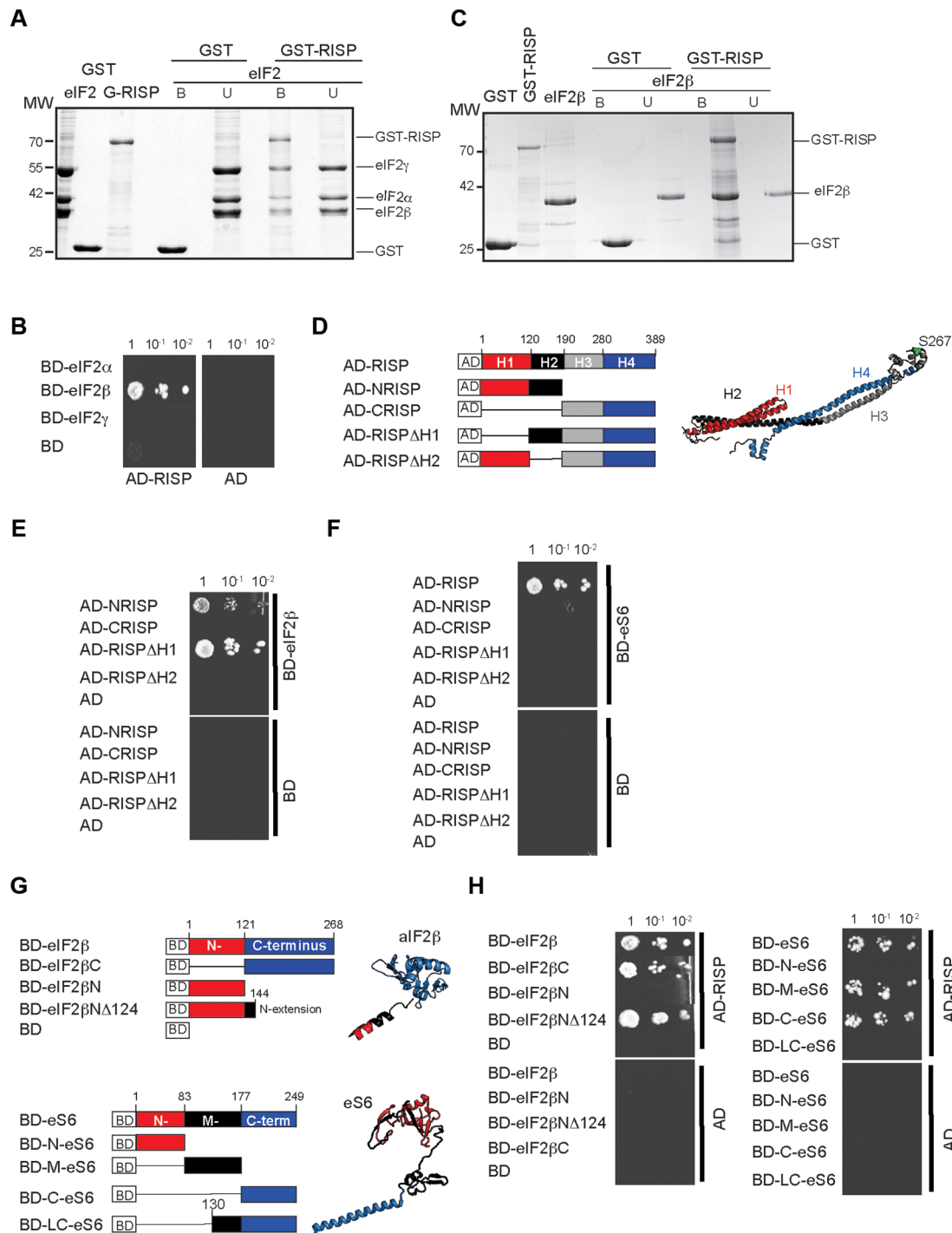
Figure 1. Mapping of interacting regions. (**A**) GST pull-down experiment using GST, GST-RISP and wheat germ-purified eIF2. GST-, GST-RISP-bound (B) and unbound (U) samples were examined by SDS-PAGE/ Coomassie staining. (**B**) Yeast two hybrid (Y2H) interactions of eIF2 subunits α, β and γ fused to Gal-4 binding domain (BD) with either activation domain (AD) or AD-RISP. Equal OD_{600} units and 1/10 and 1/100 dilutions were spotted from left to right. (**C**) eIF2β was incubated with GST- or GST-RISP-glutathione beads. eIF2β, GST and GST-RISP were expressed and purified from *E. coli*. GST-, GST-RISP-bound (B) and unbound (U) samples were examined by SDS-PAGE/ Coomassie staining. (**D**) Putative RISP 3D-structure generated by RaptorX reveals α-helixes: *red* H1, *black* H2, *grey* H3 and *blue* H4 (*right panel*). The S267-P position is indicated. RISP deletion derivatives fused to AD are depicted as boxes according to the color-code depicted in right panel. (E, F) Y2H interactions of RISP deletion derivatives fused to AD (**D**) with either BD or BD-eIF2β (**E**) and BD or *Arabidopsis* 40S ribosomal protein S6 (eS6) fused to BD (**F**). (**G**) *top right* Archaeal eIF2β (aIF2β) 3D-structure highly similar to that of the *Arabidopsis* eIF2β sequence except for a 114 N-terminal amino acid extension: *blue* C-terminus homologous to *At*eIF2βC (aa 121–268); *black* central helix corresponding to aa 121–144 of *At*eIF2β; *red* N-terminal domain. *bottom right* eS6 3D-structure in a ribosome-bound conformation. *bottom left red* N-terminal-ribosome bound domain; *black* central domain; *blue* C-terminal α-helix. eIF2β (*top left*) and eS6 (*bottom left*) deletion derivatives fused to BD are depicted as boxes according to the color-code. (**H**) Y2H interactions of AD-RISP and AD with either BD or eIF2β deletion derivatives fused to BD (*left panel*) and BD or eS6 deletion derivatives fused to BD (*right panel*).
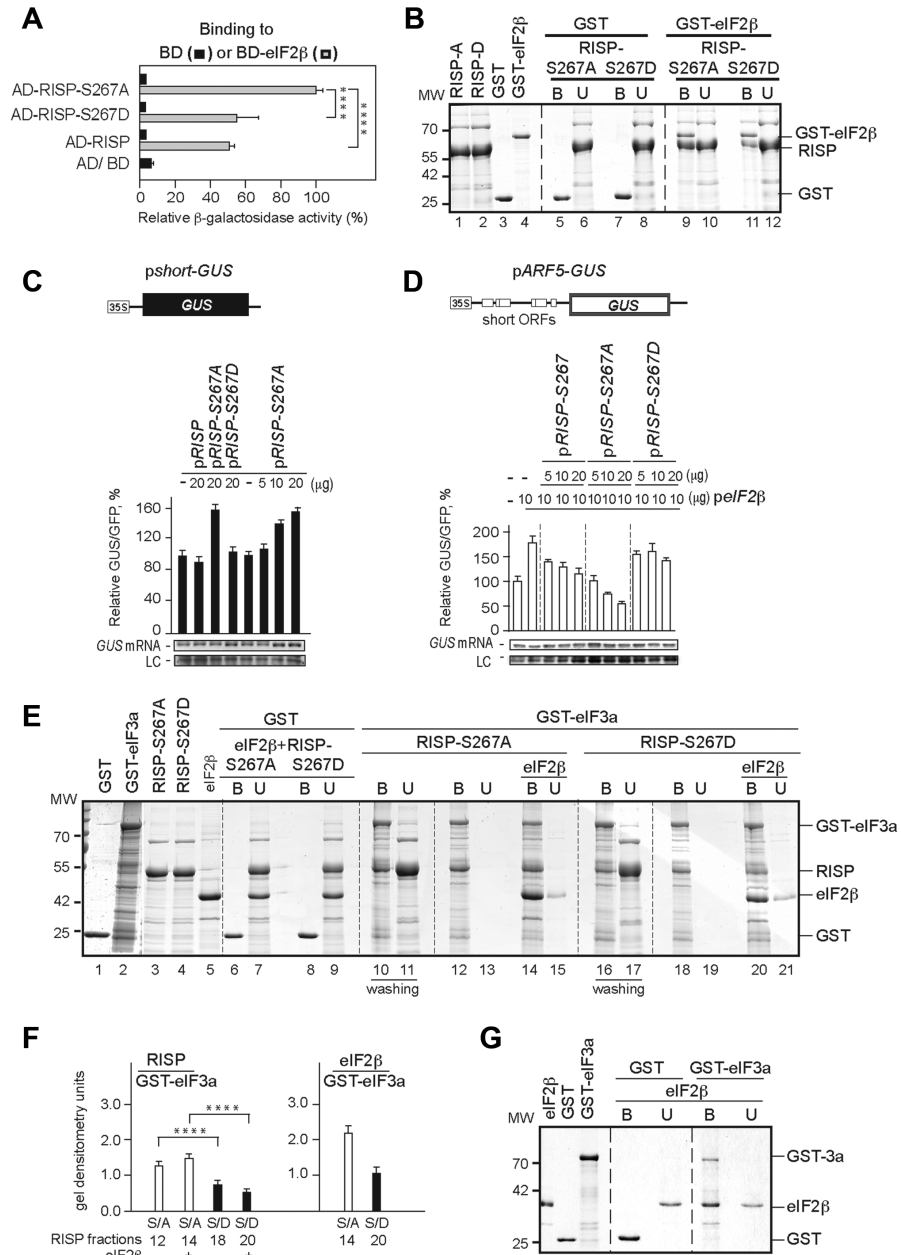
Figure 2. Interactions between eIF2β and eIF3a with RISP in different phosphorylation states. (**A**) BD-eIF2β interaction with AD-RISP, AD-tagged RISP phosphorylation knockout (AD-RISP-S267A), AD-tagged RISP phosphomimetic mutant (AD-RISP-S267D) by quantitative β-galactosidase activity liquid assay. The highest value of β-galactosidase activity with AD-RISP-S267A value set to 100%. Multiple comparisons (Turkey's test) are based on one-way ANOVA test. Data are presented as mean and error bars indicate SD (****$P < 0.0001$, $n = 3$). (**B**) His-tagged RISP-S267A (RISP-A), RISP-S267D (RISP-D) were incubated with GST- or GST-eIF2β-glutathione beads. Unbound (U) and bound (B) samples were examined by SDS-PAGE and Coomassie staining. All the experiments were reproduced at least two times with similar results. (C, D) *upper panels* Scheme of reporter plasmids used in transient expression experiments in *Arabidopsis* suspension protoplasts: (**C**) p*short-GUS* (harbors 50-nt 5′-UTR, marker for initiation efficiency) and (**D**) p*ARF5-GUS* (marker for reinitiation efficiency). uORFs within ARF5 5′-UTR are depicted as open boxes. All transformation experiments included the p*monoGFP* (marker for transformation efficiency) and either p*short GUS* (**C**) or p*ARF5-GUS* (**D**) without or with the effector plasmids that encode RISP or RISP phosphorylation mutants or eIF2β in amounts indicated above the panel. Functional levels of GUS expressed from p*short-GUS* or p*ARF5-GUS* normalized to corresponding GFP levels were set at 100%. GUS-containing mRNA levels and integrity were analyzed by sqRT–PCR; LC—loading control. Results shown represent the means obtained in three independent experiments. (**E**) GST pull-down experiments with RISP phosphorylation mutants pre-bound to GST- or GST-eIF3a-glutathione beads. After removal of unbound RISP variants GST-eIF3a-RISP-S267A (fraction 10) and GST-eIF3a-RISP-S267D (fractions 16) were further incubated without or with His-eIF2β, respectively. U and B fractions were assayed by SDS-PAGE and stained with Coomassie blue. GST, GST-eIF3a, His-RISP-S267A, His-RISP-S267D and His-eIF2β were overexpressed in *E. coli* and purified by affinity chromatography (*left panel*). (**F**) Densitometric quantification of binary (His-RISP mutant/GST-eIF3a) and ternary (eIF2β/ GST-eIF3a-RISP mutant) complexes. Values, expressed in arbitrary densitometric units, are averages of three different measurements from two biological replicates and error bars indicate SD. (**G**) eIF2β was incubated with GST- or GST-eIF3a-bound glutathione beads. eIF2β, GST and GST-eIF3a were expressed and purified from *E. coli*. GST-, GST-eIF3a-bound (B) and unbound (U) samples were examined by SDS-PAGE/ Coomassie staining. All the experiments were reproduced at least two times with similar results.

terminus, and a short central α-helix (aa 121–144) that is also present within aIF2β. Figure 1H shows that eIF2β-C binds RISP as strongly as full-length eIF2β, while the N-terminus (aa 1–121) does not. However, elongation of the eIF2β N-terminal fragment by an additional 23 aa (aa 1–144; eIF2β-NΔ124) restored the interaction, indicating that a segment spanning residues 121–144 is involved in RISP binding. Thus, results from the Y2H system suggest that the C-terminus of eIF2β is involved in RISP binding.

eIF2 and eIF3 remain as well-established members of the 43S PIC and as fundamental players in cap-dependent translation initiation. Consequently, RISP may participate in several interactions within the surroundings of eIF3a, eIF3c and eIF2β on the 40S of the 43S PIC. Note that our *in vitro* studies indicated that RISP binding to eIF3c and eL24 might reflect changes in its phosphorylation status in response to TOR activation (33).

To examine eS6 domains required for RISP binding, we took an advantage of the known 3D conformation of 40S-bound eS6 (47; Figure 1G). eS6 was dissected into three fragments. Two fragments of eS6—the central fragment, M-S6 (aa 83–177) and the C-terminal alpha-helix, C-eS6 (aa 177–249)—bind RISP as strongly as the full-length protein (Figure 1H, right panel); however, the longer C-terminal fragment of eS6, LC-eS6 (aa 130–249) failed to interact with RISP, indicating that the RISP binding site is somewhat concealed by a 47-aa fragment insertion in our Y2H conditions. Thus, we investigated further RISP interaction with the eS6 C-terminus, which contains multiple S6K1 phosphorylation sites.

We also elaborated a method of high-resolution mass spectrometry to identify factors that associate globally with RISP. RISP immunoprecipitated from *Arabidopsis rispa/35S:RISP-GFPox* line transgenic for GFP-tagged RISP using anti-GFP antibodies was subjected to liquid chromatography-tandem mass spectrometry analysis (LC–MS/MS). We identified 8 out of 13 eIF3 subunits, with subunits a and c being highly represented (Supplementary Table S1; Supplementary Figure S1). Although eIF2 is a canonical member of eIF3-containing complexes and binds RISP, eIF2 subunits were not found in GFP-RISP immunoprecipitates. However, we identified TOR, already known as a direct eIF3-binding protein in mammals (48) and as an upstream effector of RISP (33).

RISP-S267A, but not RISP-S267D, preferentially interacts with eIF2β and promotes translation initiation in plant protoplasts

RISP is phosphorylated at Ser267 within the motif RGRLES—a pattern (R/KxR/KxxS/T) found in many Akt or S6K1 substrates—by S6K1 in a TOR-responsive manner, and, when phosphorylated, preferentially binds eL24 (33), suggesting that RISP phosphorylation can modulate its partner binding. Indeed, phosphorylation of mammalian S6K1 at the hydrophobic motif residue T389 regulates the interaction between S6K1 and eIF3-PIC (48): S6K1, when dephosphorylated, associates with the eIF3 complex, while S6K1 phosphorylation promotes its dissociation from the complex. Thus, we set out to character-

ize how phosphorylation of RISP modulates its binding to eIF2β.

To explore the possibility that the phosphorylation status of RISP is an important determinant of its binding activities, we constructed RISP phosphorylation mutants—the phospho-knockout mutant S267A and mimic S267D—to study their interaction with eIF2β using the Y2H quantitative β-galactosidase assay. As shown in Figure 2A, the phosphorylation-inactive mutant RISP-S267A has a reproducibly stronger interaction with eIF2β than the phosphorylation mimic RISP-S267D or wild-type RISP, which has a high phosphorylation status, when expressed in the Y2H system (33). To further investigate whether the phosphorylation status of RISP is a determinant of its binding to eIF2β, RISP-S267A or RISP-S267D phosphorylation mutants were assayed for GST-tagged eIF2β binding, and levels of RISP mutants in the GST-bound fraction were compared (Figure 2B). Here, GST-tagged eIF2β binds RISP-S267A somewhat more strongly compared with its phosphomimetic mutant. Overall, Y2H data and GST pull-down assay suggest that, *in vitro*, RISP, when non-phosphorylated, binds eIF2β preferentially.

We next tested whether the RISP phospho-knockout mutant or mimic impact translation initiation when expressed transiently. To address this question, we monitored expression of a β-glucuronidase (GUS) reporter ORF downstream of a short synthetic leader (*short GUS*) in protoplasts prepared from *Arabidopsis* suspension culture (Figure 2C). A marker of transformation efficiency—*monoGFP* with a single GFP ORF downstream of the tobacco etch virus (TEV) 5'-leader—initiates via a cap-independent mechanism (49). Under the conditions used, overexpression of RISP-S267A, but not RISP-S267D, up-regulates expression of the short leader-containing GUS reporter by at least 1.5-fold (Figure 2C). Thus, RISP-S267A can promote translation of a short leader-containing mRNA.

The GCN4 model clearly demonstrated that GTP-bound eIF2, as a part of the ternary complex with initiator tRNAi^Met, is a critical limiting factor for reinitiation (50). Accordingly, a positive effect of eIF2β on reinitiation was demonstrated in *Arabidopsis* protoplasts, transiently expressing a GUS reporter ORF downstream of the *auxin responsive factor 5 (ARF5)* leader carrying six uORFs (*ARF5-GUS*) and p*eIF2β* (Figure 2D). The impact of eIF2β on translation reinitiation of *ARF5-GUS* was nearly two-fold. Note that eIF2 is highly flexible in solution, with the β-subunit being only loosely associated (51). Accordingly, eIF2β overexpression could up-regulate the level of eIF2 intact complexes and thus increase reinitiation efficiency, or free eIF2β can increase reinitiation via binding to its cellular partners, and thus competing with holo-eIF2.

Next we studied whether RISP-S267A or RISP-S267D, when co-synthesized together with eIF2β in plant protoplasts, will interfere with the positive effect of eIF2β on reinitiation after short ORF translation. Strikingly, expression of increasing amounts of RISP-S267A, but not RISP-S267D or WT RISP, led to significant inhibition of p*ARF5-GUS* expression, suggesting that, upon expression of both eIF2β and RISP-S267A, the latter protein can sequester the subunit β alone and/or the endogenous complete eIF2 complex. Because increasing WT RISP overexpression de-

creases *ARF5-GUS* expression to a significantly lesser extent than RISP-S267A, and in fact no interference was observed with RISP-S267D overexpression, we conclude that WT RISP, and, especially, RISP-S267D display significantly lower affinities for eIF2β. Thus, the data presented above provide *in vivo* evidence that the phosphorylation-inactive state of RISP governs its binding to eIF2-PIC via eIF2 subunit β.

The RISP phospho-knockout form might efficiently integrate into eIF3 and eIF2 complexes *in vitro*

During the step of ternary complex recruitment into the 43S PIC, interaction between eIF3 and eIF2 plays an important role (52,53). Indeed, physical interaction between eIF2 and eIF3 has been suggested in yeast (52) and *in planta* (53), and cryo-electron microscopy has allowed visualization of contacts between mammalian eIF3 and eIF2 in the 43S PIC context (5). However, it is unclear whether the preferential binding of RISP-S267A to eIF3c described in (33) is sufficient to improve recruitment of eIF2 during translation initiation, or if additional direct contact between RISP-S267A and eIF2 is required. As *in vivo* proof of this hypothesis is difficult to obtain due to essential nature and/or redundancy of eIFs, we therefore asked if non-phosphorylated RISP can form part of the eIF2-eIF3 complex *in vitro*. We performed a GST pull-down assay to investigate whether GST-tagged eIF3a, which can also bind eIF2β (as assessed *in vitro*; Figure 2G), is able to associate with RISP at different phosphorylation states in the presence of excess of eIF2β (Figure 2E).

Thus, GST-eIF3a bound to glutathione beads was incubated with excess RISP, in either phosphorylation knockout or mimic form, followed by extensive washing of unbound RISP mutants (Figure 2E; lanes 10 and 16, respectively). Next, equal amounts of glutathione beads bound to GST-eIF3a/RISP-S267A or GST-eIF3a/RISP-S267D were further incubated with or without eIF2β. After washing, bound and unbound fractions were analyzed by SDS gel followed by Coomassie staining. We found that RISP-S267A binds GST-eIF3a more efficiently than RISP-S267D with or without excess eIF2β (for quantification see Figure 2F, left panel), indicating no competition between RISP and eIF2β for eIF3a binding. Accordingly, the eIF2β component was somewhat enriched in GST-eIF3a/RISP-S267A as compared with GST-eIF3a/RISP-S267D (Figure 2F, right panel). Note that neither eIF2β nor RISP variants interacted with GST alone (Figure 2E). These results suggest the possibility of complex formation between eIF3a, RISP and eIF2β. Therefore, we propose that RISP, in largely not phosphorylated form, enters the 43S PIC to assist eIF3 in eIF2 recruitment.

RISP phospho-mimetic can form a bridge between eS6 C-terminus and the 60S ribosomal subunit

As described previously, endogenous RISP specifically cosediments with fractions of 60S ribosomal subunits and 80S ribosomes, as assessed by sucrose gradient analysis (34). RISP association with 60S might be explained by its binding to eL24 via its C-terminal domain. Previously,

we demonstrated that phosphorylated RISP-S267D binds eL24 more strongly than RISP-S267A (34). Here, the Y2H protein interaction assay showed that wild-type RISP and the RISP phosphorylation mimic mutant interacted reproducibly more strongly with C-eS6 than RISP-S267A (Figure 3A).

In yeast 80S, eL24 and eS6 C-terminal domains protrude out of 60S and 40S, respectively, being in close spatial vicinity to each other (47). Note that all our attempts to reveal direct interaction between eL24 and eS6 and their deletion mutants using the Y2H system and the GST pull-down assay failed (data not shown). This was interpreted to indicate that phosphorylated RISP might be able to mediate interactions between eS6 and 60S. First, complex formation between eS6 and 60S was examined in the presence of RISP by GST pull-down assay (Figure 3B, C). We assayed whether WT RISP can mediate binding of the GST-tagged eS6 C-terminal domain to wheat germ high salt-washed 60S ribosomal subunits. GST-C-eS6 was incubated with or without RISP, and, after removal of unbound RISP, the glutathione-bound complexes were further incubated with or without wheat germ 60S ribosomal subunits as indicated (Figure 3B). Some 60S ribosomal proteins were detected in the GST-tagged C-eS6 bound fraction specifically only in the presence of RISP, indicating weak or transient interactions between RISP-bound C-eS6 and 60S (Figure 3B, cf lanes 11 and 13; see enlarged image in Supplementary Figure S2). However, these interactions were strengthened by replacement of RISP serine residue 267 with a phosphomimetic substitution (Figure 3C). Indeed, RISP phosphorylation mimic (RISP-S267D) bound to GST-C-eS6 was able to pull down 60S, as manifested by the presence of 60S ribosomal proteins in the GST-C-eS6-bound fraction (Figure 3C, lane 18). Accordingly, we did not detect 60S ribosomal proteins in the complex with GST-C-eS6-RISP-S267A or GST alone (Figure 3C, lane 12 or 6, respectively). It is noteworthy that RISP failed to bridge C-eS6 and 60S before being phosphorylated, but was able to connect the C-terminal α-helix of eS6 and 60S as a phosphorylation mimic.

It is important to emphasize that the C-terminal α-helix of eS6 that protrudes out of 40S when exposed in the ribosome-bound state can interact with non-ribosomal proteins (47,54), and RISP is a potential candidate that is consistent with the ribosomal bound configuration of eS6.

eS6 phospho-mimetics S237D, S240D and S241D are indispensable for translation reinitiation

Our *in vitro* experiments suggest that C-eS6 is able to pull-down 60S only if it is bound to RISP-S267D (Figure 3C), indicating that eS6 is critical to link 40S with 60S if RISP is phosphorylated by S6K1. We next investigated whether phosphorylation of C-eS6 in response to TOR-S6K1 relay activation would impact translation efficiency *in planta*. Phosphoproteomic analysis of the *Arabidopsis* TOR signaling network revealed three closely spaced C-terminal eS6 phosphorylation sites—S231, S237, S240/S241—responsive to the TOR inhibitors Torin-1 or AZD-8055 (55–57). The most commonly phosphorylated eS6 residue is S240 (and apparently, S241, which is difficult
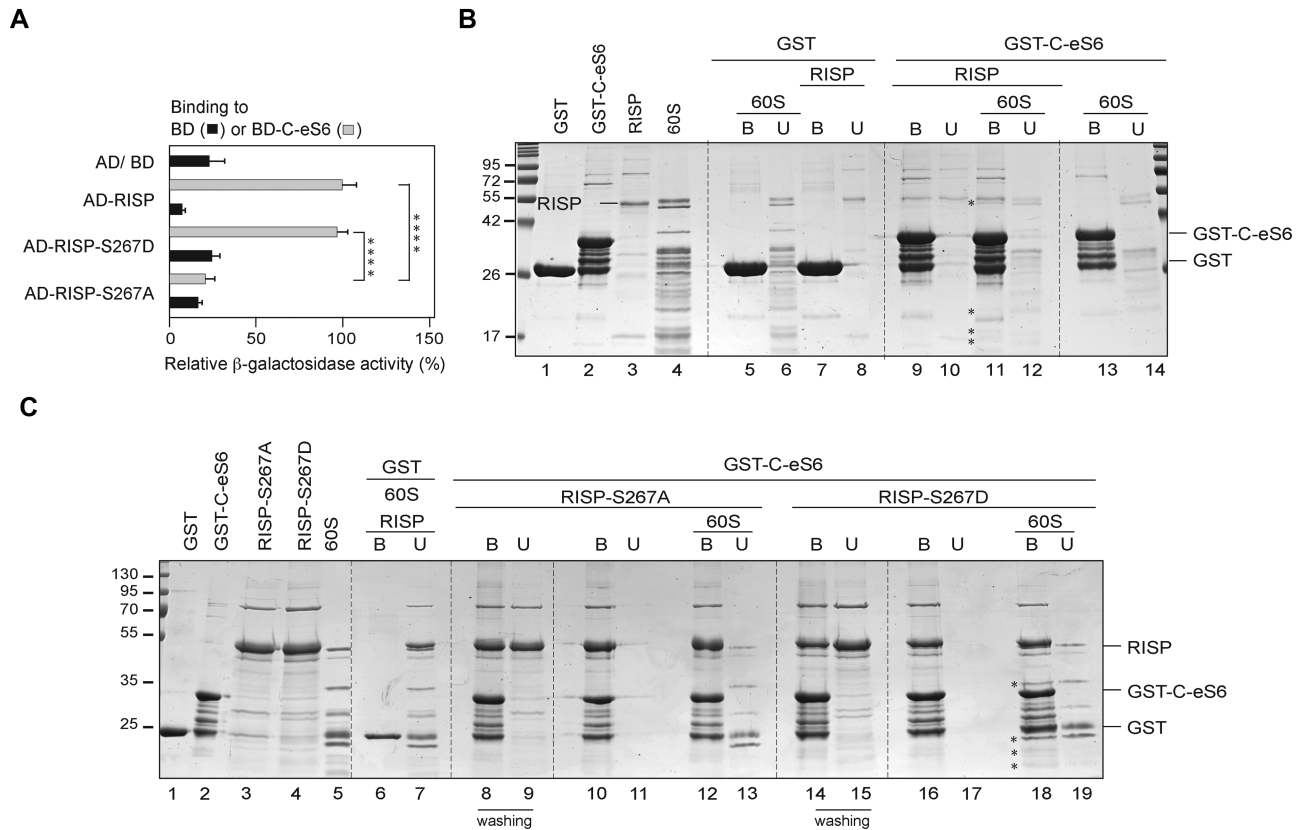
Figure 3. C-eS6-bound RISP phosphorylation mimic interacts with 60S ribosomal subunits. (**A**) BD-C-eS6 interaction with AD-RISP, AD-RISP-S267A, AD-RISP-S267D by quantitative β-galactosidase activity liquid assay. The highest value of β-galactosidase activity with AD-RISP is set to 100%. All the experiments were reproduced at least two times with similar results. Multiple comparisons (Turkey's test) are based on one-way ANOVA test. Data are presented as mean and error bars indicate SD (****$P < 0.0001$, $n = 3$). (**B**) GST-C-eS6- or GST-glutathione beads were incubated without or with WT RISP. After removal of unbound RISP, GST-C-eS6 and GST-C-eS6-RISP were further incubated with 60S as indicated above the panel. B and U samples were assayed by SDS-PAGE and stained with Coomassie blue. Stars indicate 60S ribosomal proteins specifically co-precipitated with GST-C-eS6/ RISP. (**C**) His-RISP phosphorylation mutants were incubated with GST-C-eS6 or GST-bound to glutathione beads. After removal of unbound RISP variants, GST-CS6/RISP-S267A (fraction 8) and GST-CS6/RISP-S267D (fraction 14) were further incubated without or with 60S ribosomal subunits purified from wheat germ. Unbound (U) and bound (B) samples were assayed by SDS-PAGE and stained with Coomassie blue. GST-C-eS6, RISP variants were produced in *E. coli*. Stars indicate 60S ribosomal proteins specifically co-precipitated with the GST-CS6/RISP-S267D binary complex. All the experiments were reproduced at least three times with similar results.

to distinguish from S240). First, we found that the phospho-mimetic mutants of C-eS6 at S231, or S237, or S240 more readily associated with RISP-S267D than corresponding phospho-knockout mutants (Figure 4A).

Next, we set out to determine whether phosphorylation of eS6 at the C-terminus contributes to *in planta* translation initiation or reinitiation events. *Arabidopsis* eS6 is encoded by two well-conserved genes, *RPS6A* and *RPS6B*, that encode two proteins eS6a and eS6b, respectively, having equivalent and interchangeable functions (35). We took advantage of the T-DNA insertion *rps6a* knockout mutant, where total eS6 levels were reduced to eS6b levels, and used it to obtain 35S-promoter-driven stable expression of either the eS6b phosphorylation mimic mutant (*rps6a/S6B^{S/D}*) where three closely spaced serines, S237, S240 and S241, were replaced with D (*S237D/S240D/S241D*), or the phospho-knockout mutant (*rps6a/S6B^{S/A}—S237A/S240A/S241A*). These mutant phenotypes are shown in Supplementary Figure S3. Surprisingly, 35S-promoter-driven expression of eS6b^{S/D} did not significantly restore *rps6a* developmental defects such as growth retardation, elongated and pointed

leaves when compared with expression of eS6b^{S/A}. However, we cannot exclude that extra-ribosomal functions of eS6 (58) might be perturbed by 35S-promoter-driven expression of eS6b mutants. Interestingly, the ribosomal fraction isolated from the WT *Arabidopsis* extract contains largely eS6a that is somewhat phosphorylated (Figure 4B). It is worth noting that the eS6 levels are similar in ribosomal fractions isolated from *rps6a* and WT (Figure 4B, Supplementary Figure S4), despite the total eS6b level in the *rps6a* mutant being reduced by about five-fold (35). Western blot analysis of total ribosomal fractions isolated from the homozygous lines obtained confirmed that *rps6a*, *rps6a/S6B* and *rps6a/S6B^{S/D}* express phosphorylated eS6b or eS6b^{S/D}, while, as expected, eS6b^{S/A} (*rps6a/S6B^{S/A}*) is less recognized by phospho antibodies.

In mammals, loss of eS6 phosphorylation did not alter protein synthesis rates (59), while the functional input of eS6 phosphorylation to translation is not known in plants. To determine the contribution of eS6 phosphorylation to regulating either initiation and/or reinitiation events, we used mesophyll protoplasts generated from WT
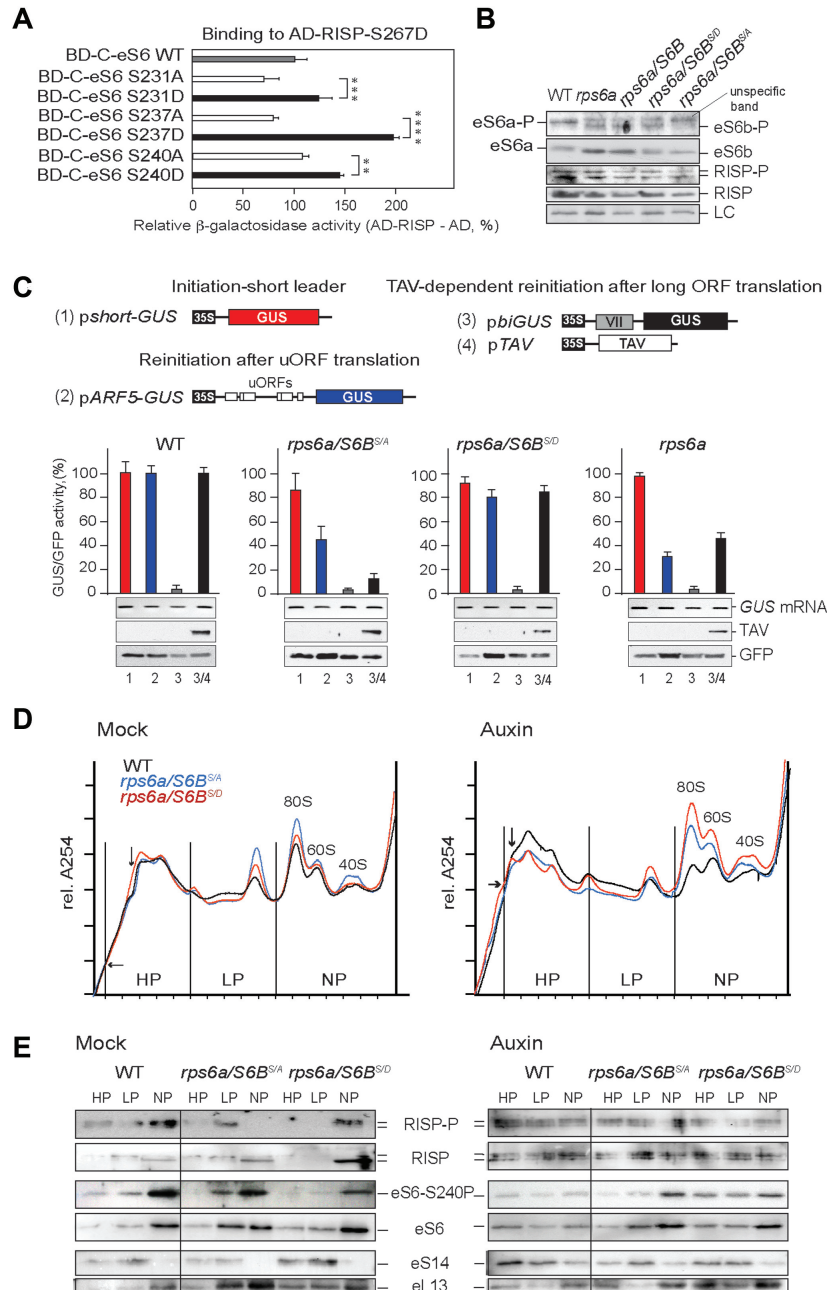
Figure 4. eS6a-deficient plants expressing the eS6b phosphomimic mutant restore efficiency of reinitiation. (**A**) AD-RISP-S267D interaction with BD-C-eS6 phosphorylation knockout mutants (C-eS6-S231A; C-eS6-S237A and C-eS6-S240A), BD-C-eS6 phosphomimetic mutants (C-eS6-S231D, C-eS6-S237D and C-eS6-S240D) by quantitative β-galactosidase activity liquid assay. The value of β-galactosidase activity with BD-C-eS6-WT and AD-RISP-S267D was set to 100%. (**B**) Western blot assessment of protein levels and their phosphorylation status (where indicated) in total ribosomal pellets from 7 days after germination (dag) WT and eS6 different genotypes (*rps6a*, *rps6a/S6B^{S/A}* and *rps6a/ S6B^{S/D}*). Proteins were separated by a 15% urea-PAGE gel and stained by Coomassie™ blue using immunoblotting with corresponding antibodies against eS6 and eS6-240-P, RISP and RISP-P. LC-loading control. (**C**) Comparable analysis of initiation and reinitiation capacities of WT, *rps6a/S6B^{S/A}* *rps6a/S6B^{S/D}* and *rps6a*. *Arabidopsis* plantlets in transient expression experiments in mesophyll protoplasts, where eS6b^{S/A} (S237A/S240A/S241A) and eS6b^{S/D} (S237D/S240S/S241D) contain triple S237/S240/S241 mutations. The 5 μg reporters—p*monoGFP* and either p*short-GUS*, or p*ARF5-GUS*, or p*biGUS* without or with p*TAV*—presented at the top were used for protoplast transformation. GUS/GFP ratios were set as 100% for each reporter plasmid in WT protoplasts. GUS/GFP activity ratios are shown in *red* (p*short-GUS*), *blue* (p*ARF5-GUS*), *grey* (p*biGUS*) and *black* (p*biGUS + pTAV*) bars. TAV and GFP protein levels were analyzed by immunoblot and shown in the bottom panels. GUS-containing mRNA levels were analyzed by semiquantitative RT-PCR. All the experiments were reproduced at least two times with similar results. Quantification represents the means ($n = 3$, error bars = SD) obtained in three experiments. (**D**) Analysis of global mRNA translation in the WT and eS6 phosphorylation mutant genotypes (*rps6a/S6B^{S/A}* and *rps6a/ S6B^{S/D}*) in mock or auxin-treated conditions. Representative polysome profiles of whole Arabidopsis extracts from 7 dag WT and eS6 phosphorylation mutant genotypes are shown. (**E**) Western blot assessment of protein levels and their phosphorylation status (where indicated) in heavy and light polysomes (HP and LP, respectively) and non-polysomal fractions (NP) of *WT*, *rps6a/S6B^{S/A}* and *rps6a/ S6B^{S/D}* genotypes. HP, LP and NP fractions were analyzed by a 12.5% SDS-PAGE gel followed by immunoblotting with antibodies as indicated (the solid line indicates removal of three *rps6a* lanes; these lanes are shown in Supplementary Figure S4B: *rps6a*).

seedlings, $rps6a/S6B^{S/A}$, $rps6a/S6B^{S/D}$ and $rps6a$ transgenic lines. Initiation events were monitored with the construct containing the GUS ORF following a short leader (p*shortGUS*), while the impact of events undergoing reinitiation after short ORF translation were followed with reporter plasmid *ARF5-GUS*, depicted in Figure 4C (upper panels). We also tested whether a special case of reinitiation after long ORF translation under control of a CaMV translation transactivator/ viroplasmin (TAV) is sensitive to the phosphorylation status of eS6. Here, we used the bicistronic reporter plasmid p*biGUS*, containing two consecutive ORFs: CaMV ORF VII and GUS, where GUS serves as a marker of transactivation, with or without the reporter plasmid expressing TAV (39) (Figure 4C).

As shown in Figure 4C (bottom panels, red bars), the levels of GUS transiently expressed from p*short-GUS* did not differ significantly in WT, $rps6a/S6B^{S/D}$ and $rps6a/S6B^{S/A}$ and $rps6a$-derived protoplasts. In contrast, translation reinitiation on *ARF5-GUS* mRNA was reduced 3-fold in $rps6a$ as compared with that in WT protoplasts, suggesting a role for eS6 in translation reinitiation (Figure 4C, blue bars). The level of reinitiation was slightly increased in $rps6a/S6B^{S/A}$, and restored in $rps6a/S6B^{S/D}$-derived protoplasts. As shown in Figure 4C (grey bars—p*biGUS*), the upstream ORF VII blocks downstream GUS ORF expression, and no GUS activity appeared in all tested protoplasts as expected. However, transfection of protoplasts with both p*biGUS* and p*TAV* resulted in the appearance of β-glucuronidase activity that was reduced about 2-fold in $rps6a$-derived protoplasts and nearly abolished in $rps6a/S6B^{S/A}$ as compared with that in WT protoplasts (Figure 4C, black bars). Strikingly, the transactivation ability of TAV decreased strongly in $rps6a/S6B^{S/A}$-derived protoplasts was fully restored in $rps6a/S6B^{S/D}$-derived protoplasts. Thus, TAV-controlled reinitiation after long ORF translation is not only eS6-dependent, but, in addition, requires eS6 phosphorylation. No significant differences in RNA transcript or TAV/GFP levels were seen in tested protoplasts. These results suggest a role for eS6 phosphorylation in plant translation reinitiation.

To estimate the effect of eS6 phosphorylation on global protein synthesis rates, we conducted polysomal profiling analyses of extracts isolated from WT seedlings, $rps6a/S6B^{S/A}$ and $rps6a/S6B^{S/D}$ transgenic lines (Figure 4D). We found no significant differences in the levels of polysomes between WT, $rps6a/S6B^{S/A}$ and $rps6a/S6B^{S/D}$, similar to previous observations in mammals. Interestingly, western blot analysis revealed that the majority of eS6b-P that resides in ribosome-containing fractions was found co-sedimented in the non-polysomal (NP) fraction, while eS14 could barely be detected in the NP fraction (Figure 4E). One explanation could be that, eS6b, whether phosphorylated or not, associates with 43S PIC, as shown in mammals (60), where eS6 interacts with the m7GpppG 5′-cap-binding complex in a casein kinase 1 responsive manner (61). Although we detected endogenous phosphorylated eS6b in NP and, to a lesser extent in LP fractions of $rps6a/S6B^{S/A}$, eS6b$^{S/A}$ is barely recognized by phospho antibodies in the heavy polysomal fraction in contrast to relatively weak, but detectable, signals in the same fraction from

WT, $rps6a/S6B^{S/D}$ (Figure 4E, left panel). Note that endogenous *ARF5* mRNA was found associated with heavy polysomes in mock controls and especially auxin-treated seedlings (29). As expected, RISP was found largely in the NP fraction, likely due to its low phosphorylation level (Figure 4E, left panel). Thus, we analyzed eS6b and RISP distribution in polyribosomes under TOR activation conditions (Figure 4E, right panel). To this end, we employed the plant hormone auxin to activate the TOR-S6K1 signaling axis and thus induce efficient loading of TOR on polysomes, phosphorylation of S6K1 and seedling reinitiation capacity (29). Crude extracts isolated from *Arabidopsis* 7 dag seedlings treated with auxin were analysed by fractionation on sucrose gradients (Figure 4D, right panel). In all polysomal profiles tested, we saw an additional heavy polyribosome peak in HP (indicated by arrows, Figure 4D). However, we observed an increased ratio between polysomes and monosomes in WT seedlings when compared with $rps6a/S6B^{S/A}$ and $rps6a/S6B^{S/D}$ genotypes, where there was a shift from polysomes to monosomes (Figure 4D), indicating less efficient formation of polysomes in both phosphomutants. Because auxin triggers TOR-S6K1-dependent phosphorylation of RISP and eS6, the level of RISP-P increased somewhat in HP fractions of all tested genotypes. Note that eS6 phosphorylation in $rps6a/S6B^{S/D}$ was significantly higher than that in $rps6a/S6B^{S/A}$ confirming that, indeed, $rps6a/S6B^{S/A}$ HP is loaded with 40S subunits lacking eS6 phosphorylation. Therefore, phosphorylation of eS6 correlates with preferential translation of uORF-containing mRNAs such as *ARF5* mRNA in $rps6a/S6B^{S/D}$, in contrast to $rps6a/S6B^{S/A}$ (Figure 4C, E). Thus, upon activation of TOR, WT and $rps6a/S6B^{S/D}$ harbour both phosphorylated RISP and phosphorylated eS6 in polysomes to stimulate reinitiation. However, there were no marked changes in the levels of heavy polysomes among $rps6a/S6B^{S/A}$ and $rps6a/S6B^{S/D}$ genotypes, strongly indicating that global protein synthesis levels were not significantly affected by non-phosphorylated isoform of eS6.

eS6-deficient plants are agravitropic and resistant to CaMV infection

Next, it was pertinent to further understand how eS6-deficient plants with defects in TAV-mediated reinitiation of translation respond to infection by CaMV, which requires the reinitiation step to achieve polycistronic translation of the 35S pregenomic RNA. Here, we examined whether eS6 deficient transgenic *Arabidopsis* plants with defects in translation reinitiation would be susceptible to CaMV infection. We took advantage of two eS6 knock-out *Arabidopsis* lines, $rps6a$ and $rps6b$ (knock-out of both genes, *RPS6A* and *RPS6B* in *Arabidopsis* is lethal), characterized by shorter primary root length compared with WT plants (Figure 5A) (35). WT, $rps6a$ and $rps6b$ were agroinfiltrated with a CaMV CM1841 infectious clone (36) at the earlier eight-leaf state. Out of 36 WT or $rps6a$ or $rps6b$ plants challenged by CaMV, 100% of WT, 70% of $rps6b$ and only 50% of $rps6a$ plants were infected (Figure 5B). While nearly 100% of WT plants displayed strong symptoms at 25 dpi, symptomatic $rps6b$ plants showed only mild vein-clearing patterns, and >50% of $rps6a$ plants displayed no signs of infection ($rps6a$ N),
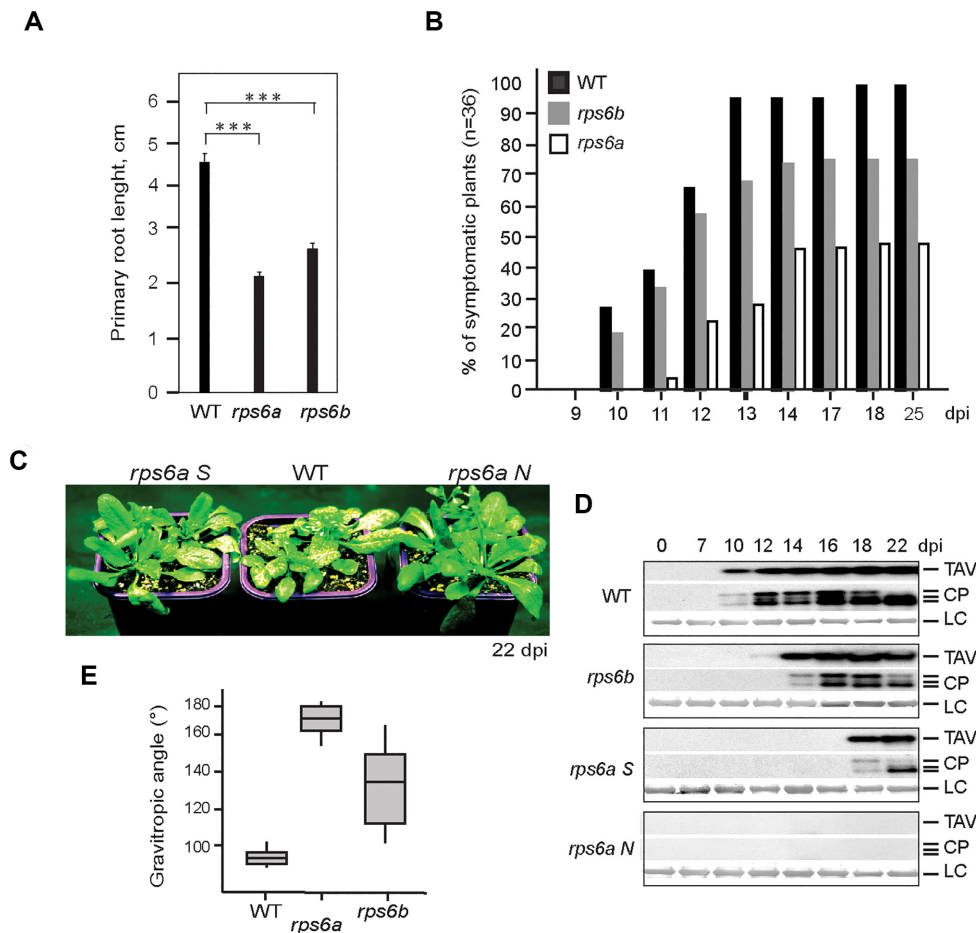
Figure 5. eS6 deficient plants confer some resistance to CaMV infection. (**A**) 7 dag *Arabidopsis* WT and eS6-deficient seedlings (*rps6a* and *rps6b*) were assayed by primary root length measurements. (**B**) Kinetics of CaMV symptom appearance in WT, eS6a and eS6b-deficient plants. (**C**) *rps6a* and WT CaMV infected plants. *rps6a* symptomatic (S) and symptom-less (N) plants (22 dpi) are shown. (**D**) Kinetics of TAV and coat protein (CP) accumulation in CaMV-infected WT, *rps6b* and *rps6a* symptomatic (S) and symptom-less (N) plants. (**E**) 7 dag *Arabidopsis* WT, *rps6a* and *rps6b* were assayed by gravitropic analysis. Curvature in root gravitropic response was analyzed 24 h after gravity stimulation. Data are means ± SD (*n* = 50).

with the remainder displaying only mild symptoms (*rps6a S*) up to 25 dpi (Figure 5C; Supplementary Figure S5), suggesting high resistance of *rps6a* plants to CaMV. Consistently, TAV and viral coat protein (CP) accumulation was first observed at 10 dpi for the majority of WT plants, at 14 dpi on average for *rps6b*, but only at 18 dpi for *rps6a* S (Figure 5D). No viral proteins were detected for *rps6a N* plants. These results strongly suggest significant downregulation of CaMV replication in plants underexpressing eS6. We concluded that this partial resistance to CaMV is due to low eS6 availability limiting viral replication in *Arabidopsis* plants.

Our and other observations suggest that known reinitiation defects associate with altered gravitropic responses (17,29). Here, we show that 8-dag *rps6b* displayed gravitropic defects after 24 hours of 90° gravity stimulation, while 8-dag *rps6a* seedlings are nearly agravitropic, as shown by the absence of bending angle after 24 h of 90° gravity stimulation (Figure 5E). Thus, we concluded that these results also indicate defects in translation reinitiation mechanisms in eS6-deficient plants.

DISCUSSION

Recent advances in genomic sequencing and high throughput translatome analysis have discovered many proteins that play accessory roles in translation, but how these proteins impact the cell translation machinery remains to be investigated. Reinitiation supporting protein (RISP) was discovered and characterized as a cofactor of the Cauliflower mosaic virus (CaMV) translational transactivator/viroplasmin (TAV) involved in translation of the viral 35S pregenomic mRNA (34). RISP, when phosphorylated by the TOR-S6K1 relay, is recruited by TAV to overcome cellular barriers to reinitiation by promoting a rare mechanism of reinitiation after long ORF translation operating on the 35S polycistronic mRNA (31). RISP is an example of a cellular scaffold protein, which, due to its four putative coiled-coil structural domains, can interact with multiple components of the cell translation machinery, although the mechanism of RISP function in translation reinitiation remains largely unknown.

Here, we propose that RISP function in translation is orchestrated by at least several components of the cell trans-

lation machinery, which we can cluster as 43S PIC components eIF2 (this study) and eIF3 (34); and as a 40S ribosomal protein S6 (eS6; this study) and 60S eL24 (19,34), via their C-terminal ends, which protrude out of the corresponding subunits facing each other within the eukaryotic 80S ribosome (47,62). In addition, we suggest that phosphorylation of S267 potentiates RISP binding to eS6, whereas RISP-P association with eIF2β is reduced. In contrast, the RISP phospho-knockout mutant, RISP-S267A, binds eIF2β more readily than eS6. Taking into account the previously demonstrated interactions of RISP-S267A with eIF3c, and RISP-S267D with eL24 (33), we assume that nonphosphorylated RISP can integrate into the 43S PIC, while RISP phosphorylation strengthens its binding to 40S and 60S. Although S267 may not be a critical interface for interaction with its multiple partners, phosphorylation of RISP may trigger conformational rearrangements that weaken the association with eIF3 and eIF2, and strengthen alternative interactions such as eL24 and eS6. In addition, phosphorylation can fine-tune protein–protein interactions via modulation of their ionic contacts. Indeed, in mammals, active TOR or inactive S6K1 interact readily with eIF3, but dissociate if their phosphorylation status is changed (48). Similarly, dynamic polysomal association or dissociation of TOR and S6K1, respectively, depending on phosphorylation status, was demonstrated in *Arabidopsis* (29). Thus, following auxin stimulation leading to TOR activation, RISP-P can bind eS6 and the 60S ribosomal subunit, which correlates with promotion of reinitiation by eS6, when phosphorylated at S237/S240/S241 *in planta*. Taking into account the above-mentioned interaction between RISP-P and eL24 (33), and the specific formation of the ternary complex eS6/RISP-P/60S *in vitro*, it may happen that RISP 'bridges' 40S and 60S during reinitiation of translation in response to TOR-S6K1 relay activation. It is worth noting that CaMV TAV binds to and activates TOR followed by activation of reinitiation after long ORF translation. Hence eS6-deficient *Arabidopsis* plants are more resistant to CaMV, consistent with a role for eS6 in viral TAV-dependent polycistronic translation.

eIF2 is primarily responsible for initiator tRNA delivery to the 43S complex. Consequently, eIF3 can promote eIF2 recruitment indirectly via eIF5, which bridges eIF3c with eIF2β in yeast and mammals (63,64,52), and directly when eIF2β binds eIF3c in yeast and plants (52,53,65) and eIF3a in yeast (66). According to our results, RISP targets eIF2β via the H2 domain, and, as it was previously shown, the same RISP H2 domain serves as a docking site for the eIF3 complex—eIF3b and eIF3c (34). Moreover, eIF3a binds eIF2β *in vitro* (Figure 2G) similar to the yeast system. Taking into account the known architecture of the 43S PIC (5), the 48S-open/closed PIC (67) and the 40S•eIF1•eIF3 complex (68), RISP is possibly located in close proximity to both eIF3a and eIF3c on 40S in a position that is well adapted for eIF2β capture into the 43S complex. Our observation that formation of the eIF3a-RISP-eIF2β ternary complex *in vitro* can proceed without eIF3a-RISP complex disruption upon eIF2β binding has further significance for our hypothesis (Figure 2E). Moreover, overexpression of RISP-S267A promotes translation of a short leader-containing mRNA in plant protoplasts (Figure 2C). Although RISP,

when pre-bound to eIF3, can enter the translational machinery at the 43S PIC formation step via binding to 40S (19), within the 43S PIC, RISP can assist eIF3 in stabilization and/or recruitment of the eIF2•GTP•Met-tRNAi^Met ternary complex by anchoring eIF2.

Plant reinitiation efficiency depends on uORF elongation rates, various initiation factors and the intercistronic distance, suggesting that underlying molecular mechanisms of reinitiation after uORF translation are conserved in eukaryotes (69). Here, overexpression of eIF2β promotes translation reinitiation of the *ARF5* leader-containing mRNA, suggesting that eIF2/eIF2β availability is the critical factor in reinitiation. It should be stressed that drop in ternary complex (TC) levels caused by eIF2 inactivation by several stress-induced kinases leads to reversible inhibition of translation reinitiation and triggers the integrated stress response (ISR) in mammals and yeast (70). Here, the phosphorylated eIF2α subunit is trapped by a multisubunit guanine nucleotide exchange factor, eIF2B, thus causing a sharp decrease in the amount of active TC (4). In plants, the only one known eIF2α kinase, GCN2 (general control non-derepressible-2 kinase) targets a similar serine residue in plant eIF2α and reduce large polyribosome complexes in response to amino acid and purine starvation (71,72), indicating that phosphorylation of eIF2α carry out important roles in the regulation of translation. Nevertheless, molecular roles of eIF2B in plant translation control remain to be determined, as the affinity of wheat eIF2 for GDP is only 10 times higher than that for GTP (73,74). Note that eIF2B genes with similarity to mammalian eIF2B subunits and eIF2Bγ and eIF2Bσ phosphopeptides were identified in *Arabidopsis*, indicating that the eIF2B complex is produced and posttranslationally modified (3). However, it remains to be seen whether eIF2B regulates reinitiation after uORF translation *in planta*.

Interestingly, in contrast to the eIF3-RISP complex, which can capture eIF2 and facilitate recruitment of the ternary complex in plants, the reinitiation accessory factors DENR-MCTS-1 can promote reinitiation after short uORF translation independently of eIF2 ternary complex abundance in *Drosophila* and humans (24,25). Although the DENR-MCTS-1 complex is not required for conventional initiation events, it can assist recycling by promoting dissociation of deacylated tRNA and mRNA from post-termination complexes (10).

Based on our GFP-RISP-bead MS–MS analysis, RISP is present as a complex with eIF3 and TOR (Supplementary Table S1), indicating the possibility of RISP phosphorylation directly within polysomes and TOR-containing eIF3 initiation complexes (29), as suggested in mammals (48). eS6 contains highly conserved serines at the C-terminus that are phosphorylated by S6Ks and RSKs in mammals (75). eS6 phosphorylation in response to TOR activation is thought to regulate global translation, including translation of mRNAs having a 5′ terminal oligopyrimidine tract (TOP mRNAs) (76). In contrast, rpS6P–/– knock-in mice with five serines of eS6 mutated to alanines is characterized by rather increased global translation, while showing no change in TOP mRNA regulation (75). Thus, the role of eS6 phosphorylation in translation remains elusive. However, phospho-eS6 can control translation of a selective sub-

class of mRNAs in a specific brain region (77), indicating that phospho-eS6, rather than regulating rates of global protein synthesis, plays a role in modulating the translation of specific mRNAs. In plants, phosphorylation, and thus activation of S6K1 correlates with eS6 phosphorylation (78,79,55). As in other eukaryotes, our experiments suggest that global protein synthesis is not significantly altered by the phosphorylation status of eS6, while eS6 phosphorylation promotes translation of mRNAs that harbor uORFs within their leader regions in plant protoplasts (Figure 4C). Hence eS6 can participate in TOR-responsive events that do not involve canonical cap-dependent initiation, but are dependent on 60S recruitment.

Both types of reinitiation, i.e. reinitiation after short ORF translation and TAV-mediated reinitiation after long ORF translation, seem to suffer in *rps6a/S6B^{S/A}* plants enriched in eS6 phospho knockout S237A, S240A and S241A (Figure 4C). A restore of both types of reinitiation can occur exclusively upon *rps6a* complementation with an eS6b phosphomimetic mutant. Reinitiation generally is suppressed in eukaryotes, and, thus, it is not surprising that *rps6a/S6B^{S/D}*, which displays increased reinitiation competency, expresses a more severe phenotype as compared with *rps6a/S6B^{S/A}* (Supplementary Figure S3). Similarly, total protein synthesis levels were also downregulated by eS6 phosphorylation in mouse embryo fibroblasts (59). However, we can not exclude that extra-ribosomal functions of eS6 might be perturbed by 35S-promoter-driven expression of eS6b (58). Thus, we discovered that eS6 can function in translation of a specific set of mRNAs that harbor uORF-containing leaders such as *ARF5* mRNA (17,80). Reinitiation after short ORF translation is an important mechanism in eukaryotes, where many repressor uORFs are implicated in the translational control of plant meristem maintenance (81) and responses to auxin (21). In plants, reinitiation persists by a mechanism that relies on activation of TOR (29,30).

The results of our study allow us to postulate a tentative model (Figure 6A) for the functional role of RISP in translation initiation and reinitiation. Under cellular conditions, TOR-S6K1 phosphorylation is maintained at a relatively low level in *Arabidopsis* (29). The unphosphorylated form of RISP is preferentially recruited to the 43S PIC as a complex with eIF3 (33), where it participates in ternary complex recruitment via eIF2. The fraction of phosphorylated RISP associated with eL24 that resides in 60S, binds the eS6 C-terminus that is exposed within the 40S interface, therefore bridging 60S and 40S ribosomal subunits (Figure 6A). Upon TOR-S6K1 signaling axis activation, eS6 and 60S-bound RISP are further phosphorylated and their interaction strengthened, improving 60S retention by the 40S ribosomal subunit (Figure 6A). One possibility is that the bridge could promote tethering of 60S by scanning 40S and, finally, its reuse for the next initiation event. In mammals, it was also proposed that 80S ribosomes rather that 40S ribosomal subunits can scan bidirectionally and reinitiate in a reconstituted translation system (13). Note that yeast eL24 is required for 60S and 40S joining (82), eL24 depletion causes the appearance of 'half-mers', when polysomes are deficient in active 60S subunits (82,83). In addition, eL24 overexpres-
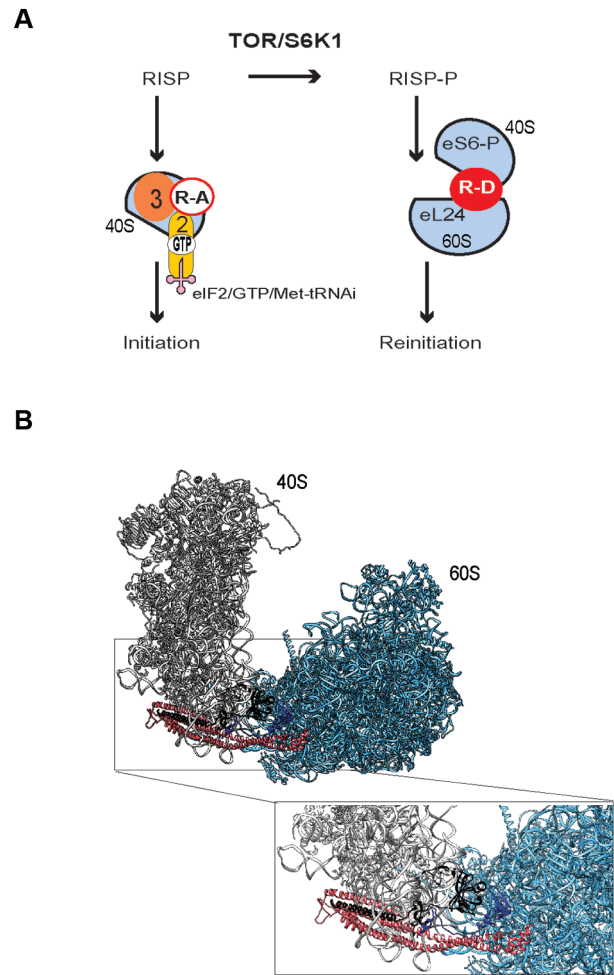
Figure 6. Model of RISP function in translation before and after phosphorylation by the TOR/S6K1 relay. (**A**) When non-phosphorylated, RISP binds eIF3 to join 40S and facilitate TC recruitment via eIF2 capture. After phosphorylation by TOR/S6K1 signaling axis, RISP can form a complex with eS6 and 60S to bridge 40S and 60S ribosomal subunits. RISP phospho-knockout mutant (R-A), RISP phospho-mimetic mutant (R-D), TC, eIF3, TOR, S6K1 are indicated. (**B**) Schematic presentation of the putative interaction model (close-up front view) between RISP and the 40S-60S posttermination scanning complex (to build putative 80S open conformation, 60S body was rotated away from 40S by 30°). 80S shows the atomic structure of 40S (in *grey*) and 60S (in *blue*) from the yeast 80S ribosome (47). The predicted RISP model was docked with no clash in close proximity to eS6 (*black*) and eL24 (*dark blue*) C-terminal helixes.

sion drastically increased TAV-mediated transactivation of polycistronic translation in plant protoplasts (19), perhaps by increasing the fraction of eL24 containing 60S.

According to the crystal structures of the 80S ribosome, the C-terminal α-helix of eS6, which harbors multiple TOR/S6K1 phosphorylation sites, protrudes towards to 60S, while eL24 protrudes out of 60S to form a new interaction site on the 40S subunit with eS6 and 18S rRNA (47,54). 40S and 60S are connected by an eB13 bridge formed by the central segments of eL24 and eS6 within the 80S ribosome, and their C-terminal segments protrude from the 80S ribosome and thus remain solvent-exposed. Here, we propose a variant of the open 80S conformation generated based on

cryo-EM data of the yeast 80S ribosome (47), where subunits are tethered together by RISP, which putative model was generated by RaptorX (45), linking the C-terminal ends of ribosomal subunits eS6 and eL24 (Figure 6B).

Our hypothesis of 60S retention during the reinitiation process correlates with *in vitro* data suggesting the crucial importance of ribosome splitting at the termination step to allow specific recognition of downstream AUG codons in yeast. A ribosome recycling factor, ABCE1 (84) plays a critical role in 60S recycling, and is positioned close to the main factor binding site in proximity to eL24, thus posing the question of whether RISP binding would interfere with its function.

The CaMV TAV protein, together with its cofactor RISP, is required to allow repeated reinitiation events during translation of polycistronic viral mRNA (34). Strikingly, both TAV and RISP can interact with eL24, where RISP binds at the C-terminus and TAV—at the N-terminus of eL24—thus establishing strong binding to 60S. Taking into account data presented here, RISP can also reach eS6 via its C-terminal tail, which protrudes away from the 40S surface. Moreover, 80S reinitiation is highly consistent with the structure of the 35S RNA, where long ORFs are tightly packed on the coding DNA strand, with very short intergenic regions, or a few aminoacid codons overlapping in different reading frames (for example, AUGA). Therefore, TAV-mediated reinitiation of translation is most likely independent of TC concentrations. While taking into account that TAV maintains high levels of active TOR and eIF3 in polysomes of CaMV infected or TAV transgenic plants, the polysome-associated eIF3-containing complex can reacquire TC during elongation or termination of translation. Finally, our results confirm significant down-regulation of CaMV replication in *Arabidopsis thaliana* lacking the *eS6a* isoform. In general, data presented in this manuscript and by others (85) indicate that plants underexpressing eS6 are less accessible for viruses that employ alternative initiation mechanisms such as polycistronic translation via reinitiation (CaMV), or cap-independent mechanisms of initiation (*Turnip mosaic virus* and *Tomato bushy stunt virus*), with both mechanisms suffering from a deficit of the canonical initiation pathway required for 60S recruitment (85).

Phosphoproteomic studies in *Arabidopsis* suggest significant quantitative increase in phosphorylation state of both eS6a and eS6b proteins in response to high CO_2 light, auxin and cytokinin availability (86–89), and a positive effect of auxin on reinitiation of translation was demonstrated (29). Here, phosphorylation of eS6, which has attracted much attention since its discovery, seems to be important in plant translation reinitiation. Obviously, further work on the functional consequences of eS6 phosphorylation in translation reinitiation is needed to better understand reinitiation mechanisms, and to uncover other layers of eS6 function in translation under the control of TOR, and many of these are yet to be explored in eukaryotes and explained at the molecular level.

DATA AVAILABILITY

All datasets generated for this study are included in the manuscript and/or the Supplementary Files.

SUPPLEMENTARY DATA

Supplementary Data are available at NAR Online.

REFERENCES

1. Jackson,R.J., Hellen,C.U.T. and Pestova,T.V. (2010) The mechanism of eukaryotic translation initiation and principles of its regulation. *Nat. Rev. Mol. Cell Biol.*, **11**, 113–127.
2. Merrick,W.C. and Pavitt,G.D. (2018) Protein synthesis initiation in eukaryotic cells. *Cold Spring Harb. Perspect. Biol.*, **10**, a033092.
3. Browning,K.S. and Bailey-Serres,J. (2015) Mechanism of cytoplasmic mRNA translation, *Arab. Book Am. Soc. Plant Biol.*, **13**, e0176-39.
4. Hinnebusch,A.G. (2006) eIF3: a versatile scaffold for translation initiation complexes. *Trends Biochem. Sci.*, **31**, 553–562.
5. des Georges,A., Dhote,V., Kuhn,L., Hellen,C.U.T., Pestova,T.V., Frank,J. and Hashem,Y. (2015) Structure of mammalian eIF3 in the context of the 43S preinitiation complex. *Nature*, **525**, 491–495.
6. Flynn,A., Oldfield,S. and Proud,C.G. (1993) The role of the β-subunit of initiation factor eIF-2 in initiation complex formation. *Biochim. Biophys. Acta BBA - Gene Struct. Expr.*, **1174**, 117–121.
7. Huang,H., Yoon,H., Hannig,E.M. and Donahue,T.F. (1997) GTP hydrolysis controls stringent selection of the AUG start codon during translation initiation in Saccharomyces cerevisiae. *Genes Dev.*, **11**, 2396–2413.
8. Lee,A.S.Y., Kranzusch,P.J., Doudna,J.A. and Cate,J.H.D. (2016) eIF3d is an mRNA cap-binding protein that is required for specialized translation initiation. *Nature*, **536**, 96–99.
9. Kumar,P., Hellen,C.U.T. and Pestova,T.V. (2016) Toward the mechanism of eIF4F-mediated ribosomal attachment to mammalian capped mRNAs. *Genes Dev.*, **30**, 1573–1588.
10. Skabkin,M.A., Skabkina,O.V., Dhote,V., Komar,A.A., Hellen,C.U.T. and Pestova,T.V. (2010) Activities of ligatin and MCT-1/DENR in eukaryotic translation initiation and ribosomal recycling. *Genes Dev.*, **24**, 1787–1801.
11. Toribio,R., Muñoz,A., Castro-Sanz,A.B., Merchante,C. and Castellano,M.M. (2019) A novel eIF4E-interacting protein that forms non-canonical translation initiation complexes. *Nat. Plants*, **5**, 1283–1296.
12. Bruns,A.N., Li,S., Mohannath,G. and Bisaro,D.M. (2019) Phosphorylation of Arabidopsis eIF4E and eIFiso4E by SnRK1 inhibits translation. *FEBS J.*, **286**, 3778–3796.
13. Skabkin,M.A., Skabkina,O.V., Hellen,C.U.T. and Pestova,T.V. (2013) Reinitiation and other unconventional posttermination events during eukaryotic translation. *Mol. Cell*, **51**, 249–264.
14. Kozak,M. (2001) Constraints on reinitiation of translation in mammals. *Nucleic Acids Res.*, **29**, 5226–5232.
15. Wagner,S., Herrmannová,A., Hronová,V., Gunišová,S., Sen,N.D., Hannan,R.D., Hinnebusch,A.G., Shirokikh,N.E., Preiss,T. and Valášek,L.S. (2020) Selective translation complex profiling reveals staged initiation and co-translational assembly of initiation factor complexes, *Mol. Cell*, **79**, 546–560.

16. Calvo,S.E., Pagliarini,D.J. and Mootha,V.K. (2009) Upstream open reading frames cause widespread reduction of protein expression and are polymorphic among humans. *Proc. Natl. Acad. Sci. U.S.A.*, **106**, 7507–7512.

17. Zhou,F., Roy,B. and von Arnim,A.G. (2010) Translation reinitiation and development are compromised in similar ways by mutations in translation initiation factor eIF3h and the ribosomal protein RPL24. *BMC Plant Biol.*, **10**, 193.

18. Ingolia,N.T., Lareau,L.F. and Weissman,J.S. (2011) Ribosome profiling of mouse embryonic stem cells reveals the complexity and dynamics of mammalian proteomes. *Cell*, **147**, 789–802.

19. Park,H.-S., Himmelbach,A., Browning,K.S., Hohn,T. and Ryabova,L.A. (2001) A plant viral 'reinitiation' factor interacts with the host translational machinery. *Cell*, **106**, 723–733.

20. Cuchalová,L., Kouba,T., Herrmannová,A., Dányi,I., Chiu,W. and Valášek,L. (2010) The RNA recognition motif of eukaryotic translation initiation factor 3g (eIF3g) is required for resumption of scanning of posttermination ribosomes for reinitiation on GCN4 and together with eIF3i stimulates linear scanning. *Mol. Cell. Biol.*, **30**, 4671–4686.

21. Roy,B., Vaughn,J.N., Kim,B.-H., Zhou,F., Gilchrist,M.A. and Arnim,A.G.V. (2010) The h subunit of eIF3 promotes reinitiation competence during translation of mRNAs harboring upstream open reading frames. *RNA*, **16**, 748–761.

22. Munzarová,V., Pánek,J., Gunišová,S., Dányi,I., Szamecz,B. and Valášek,L.S. (2011) Translation reinitiation relies on the interaction between eIF3a/TIF32 and progressively folded cis-acting mRNA elements preceding short uORFs. *PLoS Genet.*, **7**, e1002137.

23. Weisser,M., Schäfer,T., Leibundgut,M., Böhringer,D., Aylett,C.H.S. and Ban,N. (2017) Structural and functional insights into human re-initiation complexes. *Mol. Cell*, **67**, 447–456.

24. Schleich,S., Strassburger,K., Janiesch,P.C., Koledachkina,T., Miller,K.K., Haneke,K., Cheng,Y.S., Kuechler,K., Stoecklin,G., Duncan,K.E., Teleman,A.A. *et al.* (2014) DENR–MCT-1 promotes translation re-initiation downstream of uORFs to control tissue growth, *Nature*, **512**, 208.

25. Schleich,S., Acevedo,J.M., von Hohenberg,K. and Teleman,A.A. (2017) Identification of transcripts with short stuORFs as targets for DENR•MCTS1-dependent translation in human cells. *Sci. Rep.*, **7**, 3722.

26. Ma,X.M. and Blenis,J. (2009) Molecular mechanisms of mTOR-mediated translational control. *Nat. Rev. Mol. Cell Biol.*, **10**, 307–318.

27. Saxton,R.A. and Sabatini,D.M. (2017) mTOR signaling in growth, metabolism, and disease. *Cell*, **169**, 361–371.

28. Schepetilnikov,M. and Ryabova,L.A. (2018) Recent discoveries on the role of TOR (target of rapamycin) signaling in translation in plants. *Plant Physiol.*, **176**, 1095–1105.

29. Schepetilnikov,M., Mancera-Martínez,E., Dimitrova,M., Geldreich,A., Keller,M. and Ryabova,L.A. (2013) TOR and S6K1 promote translation reinitiation of uORF-containing mRNAs via phosphorylation of eIF3h. *EMBO J.*, **32**, 1087–1102.

30. Schepetilnikov,M., Makarian,J., Srour,O., Geldreich,A., Yang,Z., Chicher,J., Hammann,P. and Ryabova,L.A. (2017) GTPase ROP2 binds and promotes activation of target of rapamycin, TOR, in response to auxin. *EMBO J.*, **36**, 886–903.

31. Fütterer,J. and Hohn,T. (1992) Role of an upstream open reading frame in the translation of polycistronic mRNAs in plant cells. *Nucleic Acids Res.*, **20**, 3851–3857.

32. Pooggin,M.M. and Ryabova,L.A. (2018) Ribosome shunting, polycistronic translation, and evasion of antiviral defenses in plant pararetroviruses and beyond. *Front. Microbiol.*, **9**, 644.

33. Schepetilnikov,M., Kobayashi,K., Geldreich,A., Caranta,C., Robaglia,C., Keller,M. and Ryabova,L.A. (2011) Viral factor TAV recruits TOR/S6K1 signalling to activate reinitiation after long ORF translation. *EMBO J.*, **30**, 1343–1356.

34. Thiébeauld,O., Schepetilnikov,M., Park,H.-S., Geldreich,A., Kobayashi,K., Keller,M., Hohn,T. and Ryabova,L.A. (2009) A new plant protein interacts with eIF3 and 60S to enhance virus-activated translation re-initiation. *EMBO J.*, **28**, 3171–3184.

35. Creff,A., Sormani,R. and Desnos,T. (2010) The two Arabidopsis RPS6 genes, encoding for cytoplasmic ribosomal proteins S6, are functionally equivalent. *Plant Mol. Biol.*, **73**, 533–546.

36. Kobayashi,K. and Hohn,T. (2003) Dissection of cauliflower mosaic virus transactivator/viroplasmin reveals distinct essential functions in basic virus replication. *J. Virol.*, **77**, 8577–8583.

37. Kobayashi,K. and Hohn,T. (2004) The avirulence domain of cauliflower mosaic virus transactivator/viroplasmin is a determinant of viral virulence in susceptible hosts. *Mol. Plant. Microbe Interact.*, **17**, 475–483.

38. Yoo,S.-D., Cho,Y.-H. and Sheen,J. (2007) Arabidopsis mesophyll protoplasts: a versatile cell system for transient gene expression analysis. *Nat. Protoc.*, **2**, 1565–1572.

39. Bonneville,J.M., Sanfaçon,H., Fütterer,J. and Hohn,T. (1989) Posttranscriptional trans-activation in cauliflower mosaic virus. *Cell*, **59**, 1135–1143.

40. Kobayashi,K., Tsuge,S., Nakayashiki,H., Mise,K. and Furusawa,I. (1998) Requirement of cauliflower mosaic virus open reading frame VI product for viral gene expression and multiplication in turnip protoplasts. *Microbiol. Immunol.*, **42**, 377–386.

41. Pooggin,M.M., Hohn,T. and Fütterer,J. (2000) Role of a short open reading frame in ribosome shunt on the cauliflower mosaic virus RNA leader. *J. Biol. Chem.*, **275**, 17288–17296.

42. Merret,R., Nagarajan,V.K., Carpentier,M.-C., Park,S., Favory,J.-J., Descombin,J., Picart,C., Charng,Y., Green,P.J., Deragon,J.-M. *et al.* (2015) Heat-induced ribosome pausing triggers mRNA co-translational decay in *Arabidopsis thaliana*. *Nucleic Acids Res.*, **43**, 4121–4132.

43. Bureau,M., Leh,V., Haas,M., Geldreich,A., Ryabova,L., Yot,Y. and Keller,M. (2004) P6 protein of cauliflower mosaic virus, a translation reinitiator, interacts with ribosomal protein L13 from Arabidopsis thaliana. *J. Gen. Virol.*, **85**, 3765–3775.

44. Chicher,J., Simonetti,A., Kuhn,L., Schaeffer,L., Hammann,P., Eriani,G. and Martin,F. (2015) Purification of mRNA-programmed translation initiation complexes suitable for mass spectrometry analysis. *Proteomics*, **15**, 2417–2425.

45. Källberg,M., Wang,H., Wang,S., Peng,J., Wang,Z., Lu,H. and Xu,J. (2012) Template-based protein structure modeling using the RaptorX web server. *Nat. Protoc.*, **7**, 1511–1522.

46. Schmitt,E., Naveau,M. and Mechulam,Y. (2010) Eukaryotic and archaeal translation initiation factor 2: a heterotrimeric tRNA carrier. *FEBS Lett.*, **584**, 405–412.

47. Ben-Shem,A., de Loubresse,N.G., Melnikov,S., Jenner,L., Yusupova,G. and Yusupov,M. (2011) The structure of the eukaryotic ribosome at 3.0 Å resolution. *Science*, **334**, 1524–1529.

48. Holz,M.K., Ballif,B.A., Gygi,S.P. and Blenis,J. (2005) mTOR and S6K1 mediate assembly of the translation preinitiation complex through dynamic protein interchange and ordered phosphorylation events. *Cell*, **123**, 569–580.

49. Zeenko,V. and Gallie,D.R. (2005) Cap-independent translation of tobacco etch virus is conferred by an RNA pseudoknot in the 5′-leader. *J. Biol. Chem.*, **280**, 26813–26824.

50. Hinnebusch,A.G. (1997) Translational regulation of yeast GCN4 a window on factors that control initiator-tRNA binding to the ribosome. *J. Biol. Chem.*, **272**, 21661–21664.

51. Beilsten-Edmands,V., Gordiyenko,Y., Kung,J.C., Mohammed,S., Schmidt,C. and Robinson,C.V. (2015) eIF2 interactions with initiator tRNA and eIF2B are regulated by post-translational modifications and conformational dynamics. *Cell Discov.*, **1**, 15020.

52. Asano,K., Clayton,J., Shalev,A. and Hinnebusch,A.G. (2000) A multifactor complex of eukaryotic initiation factors, eIF1, eIF2, eIF3, eIF5, and initiator tRNAMet is an important translation initiation intermediate in vivo. *Genes Dev.*, **14**, 2534–2546.

53. Dennis,A.G. and Browning,K.S. (2009) Differential phosphorylation of plant translation initiation factors by *Arabidopsis thaliana* CK2 holoenzymes. *J. Biol. Chem.*, **284**, 20602–20614.

54. Anger,A.M., Armache,J.-P., Berninghausen,O., Habeck,M., Subklewe,M., Wilson,D.N. and Beckmann,R. (2013) Structures of the human and Drosophila 80S ribosome. *Nature*, **497**, 80–85.

55. Dobrenel,T., Mancera-Martínez,E., Forzani,C., Azzopardi,M., Davanture,M., Moreau,M., Schepetilnikov,M., Chicher,J., Langella,O., Zivy,M. *et al.* (2016) The Arabidopsis TOR kinase specifically regulates the expression of nuclear genes coding for plastidic ribosomal proteins and the phosphorylation of the cytosolic ribosomal protein S6. *Front. Plant Sci.*, **7**, 1611.

56. Nukarinen,E., Nägele,T., Pedrotti,L., Wurzinger,B., Mair,A., Landgraf,R., Börnke,F., Hanson,J., Teige,M., Baena-Gonzalez,E.

et al. (2016) Quantitative phosphoproteomics reveals the role of the AMPK plant ortholog SnRK1 as a metabolic master regulator under energy deprivation. *Sci. Rep.*, **6**, 31697.

57. Van Leene,J., Han,C., Gadeyne,A., Eeckhout,D., Matthijs,C., Cannoot,B., De Winne,N., Persiau,G., Van De Slijke,E., Van de Cotte,B. *et al.* (2019) Capturing the phosphorylation and protein interaction landscape of the plant TOR kinase. *Nat. Plants*, **5**, 316–327.

58. Kim,Y.-K., Kim,S., Shin,Y-J., Hur,Y.-S., Kim,W.-Y., Lee,M.-S., Cheon,C.-.I. and Verma,D.P.S. (2014) Ribosomal protein S6, a target of rapamycin, is involved in the regulation of rRNA genes by possible epigenetic changes in Arabidopsis. *J. Biol. Chem.*, **289**, 3901–3912.

59. Ruvinsky,I. and Meyuhas,O. (2006) Ribosomal protein S6 phosphorylation: from protein synthesis to cell size. *Trends Biochem. Sci.*, **31**, 342–348.

60. Roux,P.P., Shahbazian,D., Vu,H., Holz,M.K., Cohen,M.S., Taunton,J., Sonenberg,N. and Blenis,J. (2007) RAS/ERK signaling promotes site-specific ribosomal protein S6 phosphorylation via RSK and stimulates Cap-dependent translation. *J. Biol. Chem.*, **282**, 14056–14064.

61. Hutchinson,J.A., Shanware,N.P., Chang,H. and Tibbetts,R.S. (2011) Regulation of ribosomal protein S6 phosphorylation by casein kinase 1 and protein phosphatase 1. *J. Biol. Chem.*, **286**, 8688–8696.

62. Khatter,H., Myasnikov,A.G., Natchiar,S.K. and Klaholz,B.P. (2015) Structure of the human 80S ribosome. *Nature*, **520**, 640–645.

63. Das,S., Maiti,T., Das,K. and Maitra,U. (1997) Specific interaction of eukaryotic translation initiation factor 5 (eIF5) with the β-subunit of eIF2. *J. Biol. Chem.*, **272**, 31712–31718.

64. Fletcher,C.M., Pestova,T.V., Hellen,C.U.T. and Wagner,G. (1999) Structure and interactions of the translation initiation factor eIF1. *EMBO J.*, **18**, 2631–2637.

65. Dennis,M.D., Person,M.D. and Browning,K.S. (2009) Phosphorylation of plant translation initiation factors by CK2 enhances the in vitro interaction of multifactor complex components. *J. Biol. Chem.*, **284**, 20615–20628.

66. Valášek,L., Nielsen,K.H. and Hinnebusch,A.G. (2002) Direct eIF2–eIF3 contact in the multifactor complex is important for translation initiation in vivo. *EMBO J.*, **21**, 5886–5898.

67. Llácer,J.L., Hussain,T., Marler,L., Aitken,C.E., Thakur,A., Lorsch,J.R., Hinnebusch,A.G. and Ramakrishnan,V. (2015) Conformational differences between open and closed states of the eukaryotic translation initiation complex. *Mol. Cell*, **59**, 399–412.

68. Erzberger,J.P., Stengel,F., Pellarin,R., Zhang,S., Schaefer,T., Aylett,C.H.S., Cimermancic,P., Boehringer,D., Sali,A., Aebersold,R. *et al.* (2014) Molecular architecture of the 40S·eIF1·eIF3 translation initiation complex. *Cell*, **158**, 1123–1135.

69. von Arnim,A., Jia,Q. and Vaughn,J.N. (2014) Regulation of plant translation by upstream open reading frames. *Plant Sci.*, **214**, 1–12.

70. Young,S.K. and Wek,R.C. (2016) Upstream open reading frames differentially regulate gene specific translation in the integrated stress response. *J. Biol. Chem.*, **291**, 16927–16935.

71. Lageix,S., Lanet,E., Pouch-Pélissier,M-N., Espagnol,M-C., Robaglia,C., Deragon,J.-M. and Pélissier,T. (2008) Arabidopsis eIF2α kinase GCN2 is essential for growth in stress conditions and is activated by wounding. *BMC Plant Biol.*, **8**, 134.

72. Zhang,Y., Wang,Y., Kanyuka,K., Parry,M.A.J., Powers,S.J. and Halford,N.G. (2008) GCN2-dependent phosphorylation of eukaryotic translation initiation factor-2α in Arabidopsis. *J. Exp. Bot.*, **59**, 3131–3141.

73. Shaikhin,S.M., Smailov,S.K., Lee,A.V., Kozhanov,E.V. and Iskakov,B.K. (1992) Interaction of wheat germ translation initiation factor 2 with GDP and GTP. *Biochimie*, **74**, 447–454.

74. Immanuel,T.M., Greenwood,D.R. and MacDiarmid,R.M. (2012) A critical review of translation initiation factor eIF2α kinases in plants - regulating protein synthesis during stress. *Funct. Plant Biol.*, **39**, 717–735.

75. Ruvinsky,I., Sharon,N., Lerer,T., Cohen,H., Stolovich-Rain,M., Nir,T., Dor,Y., Zisman,P. and Meyuhas,O. (2005) Ribosomal protein S6 phosphorylation is a determinant of cell size and glucose homeostasis. *Genes Dev.*, **19**, 2199–2211.

76. Meyuhas,O. and Kahan,T. (2015) The race to decipher the top secrets of TOP mRNAs. *Biochim. Biophys. Acta BBA - Gene Regul. Mech.*, **1849**, 801–811.

77. Puighermanal,E., Biever,A., Pascoli,V., Melser,S., Pratlong,M., Cutando,L., Rialle,S., Severac,D., Boubaker-Vitre,J., Meyuhas,O. *et al.* (2017) Ribosomal protein S6 phosphorylation is involved in novelty-induced locomotion, synaptic plasticity and mRNA translation. *Front. Mol. Neurosci.*, **10**, 419.

78. Turck,F., Kozma,S.C., Thomas,G. and Nagy,F. (1998) A heat-sensitive *Arabidopsis thaliana* kinase substitutes for human p70s6k function in vivo. *Mol. Cell. Biol.*, **18**, 2038–2044.

79. Mahfouz,M.M., Kim,S., Delauney,A.J. and Verma,D.P.S. (2006) *Arabidopsis* target of rapamycin interacts with RAPTOR, which regulates the activity of S6 kinase in response to osmotic stress signals. *Plant Cell Online*, **18**, 477–490.

80. Nishimura,T., Wada,T., Yamamoto,K.T. and Okada,K. (2005) The Arabidopsis STV1 protein, responsible for translation reinitiation, is required for auxin-mediated gynoecium patterning. *Plant Cell*, **17**, 2940–2953.

81. Zhou,F., Roy,B., Dunlap,J.R., Enganti,R. and von Arnim,A.G. (2014) Translational control of Arabidopsis meristem stability and organogenesis by the eukaryotic translation factor eIF3h. *PLoS One*, **9**, e95396.

82. Dresios,J., Panopoulos,P., Suzuki,K. and Synetos,D. (2003) A dispensable yeast ribosomal protein optimizes peptidyltransferase activity and affects translocation. *J. Biol. Chem.*, **278**, 3314–3322.

83. Baronas-Lowell,D.M. and Warner,J.R. (1990) Ribosomal protein L30 is dispensable in the yeast Saccharomyces cerevisiae. *Mol. Cell. Biol.*, **10**, 5235–5243.

84. Nürenberg,E. and Tampé,R. (2013) Tying up loose ends: ribosome recycling in eukaryotes and archaea. *Trends Biochem. Sci.*, **38**, 64–74.

85. Yang,C., Zhang,C., Dittman,J.D. and Whitham,S.A. (2009) Differential requirement of ribosomal protein S6 by plant RNA viruses with different translation initiation strategies. *Virology*, **390**, 163–173.

86. Turck,F., Zilbermann,F., Kozma,S.C., Thomas,G. and Nagy,F. (2004) Phytohormones participate in an S6 kinase signal transduction pathway in Arabidopsis. *Plant Physiol.*, **134**, 1527–1535.

87. Boex-Fontvieille,E., Daventure,M., Jossier,M., Zivy,M., Hodges,M. and Tcherkez,G. (2013) Photosynthetic control of Arabidopsis leaf cytoplasmic translation initiation by protein phosphorylation. *PLoS One*, **8**, e70692.

88. Turkina,M.V., Arstrand,H.K. and Vener,A.V. (2011) Differential phosphorylation of ribosomal proteins in *Arabidopsis thaliana* plants during day and night. *PLoS One*, **6**, e29307.

89. Carroll,A.J., Heazlewood,J.L., Ito,J. and Millar,A.H. (2008) Analysis of the Arabidopsis cytosolic ribosome proteome provides detailed insights into its components and their post-translational modification. *Mol. Cell. Proteomics*, **7**, 347–369.